Supplemental Information for:

Anthropogenic Secondary Organic Aerosols Contribute Substantially to Air Pollution Mortality

Benjamin A. Nault et al.

Correspondence: Jose L. Jimenez (jose.jimenez@colorado.edu)

Section S1 US Emission Inventories

Anthropogenic VOC emissions

The US emissions of VOCs is based on a mass balance estimate of the petrochemical industry reported by McDonald et al. (2018). Briefly, fuel sales and chemical product use are estimated from publicly available reports on energy use, chemical production, economic surveys, and freight shipments. Mobile source emission factors are from prior work quantifying both on-road and off-road engines (McDonald et al., 2013, 2015). Evaporative sources of transportation fuels are considered in addition to tailpipe exhaust (Pierson et al., 1999). VCP emission factors are based on literature values, including from the indoor environment, and reported in McDonald et al. (2018). Other fossil energy sources of VOCs, such as from oil refineries and industry, are taken from official inventories reported by the California Air Resources Board (CARB, 2013) or US Environmental Protection Agency (NEI, 2015). McDonald et al. (2018) reported fossil-VOC emissions for the Los Angeles basin in the year 2010.

Speciation of VOC emissions

The total VOC emissions are speciated to estimate BTEX and IVOC emissions from petrochemical VOC sources. Briefly, gasoline and diesel exhaust, gasoline fuel, and headspace vapors are based on profiles reported in the literature from the Caldecott Tunnel (Gentner et al., 2012, 2013). Speciation profiles of VCPs are based on California Air Resources Board surveys of architectural coatings (Davis, 2007) and consumer products (CCPR, 2015). Other industrial

solvent uses and point/area source emissions are from the EPA SPECIATE (v4.4) database (EPA, 2014).

Extrapolating IVOC/BTEX ratios from 2010 Los Angeles to other field campaigns

In the ASOA mass closure estimation, three separate field campaigns are utilized from the US: NEAQS 2002 (Boston/New York City), CalNex 2010 (Los Angeles), and WINTER 2015 (New York City outflow). These field campaigns span two megacities (Los Angeles and New York City), ~one decade, and two seasons (summer versus winter). Here, we discuss how each of these variables could affect the IVOC/BTEX emissions ratio. We focus the discussion on mobile sources and VCPs because these are the dominant contributors to BTEX and IVOCs.

The IVOC/BTEX emissions ratio could be affected by the population density of a city. It is well-established that per capita transportation fuel use decreases with increasing population density (Gately et al., 2015), whereas VCP usage is expected to scale with population. Relative to Los Angeles, the per capita fuel use in New York City is ~2 times lower (Gately et al., 2015), resulting in lower on-road transportation VOC emissions relative to VCPs. Because aromatics are mainly found in gasoline, whereas the IVOCs have a higher contribution from VCPs, the IVOC/BTEX ratio is expected to be higher in New York City than Los Angeles.

To assess impacts of annual trends on the IVOC/BTEX ratio, we utilize long-term trend analyses of mobile source VOC emissions in Los Angeles (McDonald et al., 2013, 2015; Hassler et al., 2016). The main effect is that on-road gasoline emissions have decreased with time, both from the tailpipe of vehicles (McDonald et al., 2013) and of gasoline-related VOCs in ambient air measurements (Warneke et al., 2012). We utilize the EPA Trends Report to scale VOC

emissions for other anthropogenic sectors, including VCPs and industrial sources (https://www.epa.gov/air-emissions-inventories/air-pollutant-emissions-trends-data). The EPA Trends Report suggests that VCP (or solvent) emissions decreased by ~30% between 2002 and 2010, including efforts to reduce the VOC content of architectural coatings (Matheson, 2002). After 2010, the emissions have been slightly increasing, likely due to population growth. Because both mobile sources and VCP emissions are decreasing with time, the IVOC/BTEX emissions ratio is not significantly altered.

Lastly, the effects of seasonality influence on-road transportation emissions through: (i) increased VOC emissions in winter relative to summer from cold-starting engines, and (ii) lower evaporative emissions due to colder ambient temperatures. We estimate that exhaust emissions from passenger vehicles increases by ~50% due to higher cold-start emissions in winter relative to summer based on the EPA MOVES model (MOVES, 2015). Evaporated gasoline and headspace vapors are known to exhibit a temperature-dependence (Rubin et al., 2006), and estimated to be ~20% and ~80% lower, respectively, based on typical wintertime temperatures of New York City relative to summertime Los Angeles. Due to compensating factors between cold-start engines and evaporated fuels, the IVOC/BTEX emissions are not significantly affected by seasonality.

Overall, when taking into account differences in population density between Los Angeles and New York City, trends of mobile source and VCP emissions over time, and seasonality, the IVOC/BTEX emission ratios range between ~2.3 to 2.7, which is relatively small. This sensitivity analysis helps explain why the enhancement observed in SOA scales with BTEX levels in the urban atmosphere.

73

Section S2 Beijing Emission Inventory

Anthropogenic VOC emissions

The total VOC emissions of Beijing were developed following the bottom-up framework of the Multi-resolution Emission Inventory for China (MEIC) model (available at http://www.meicmodel.org), based on a technology-based methodology. The details of activity rates, emission factors, technology distribution, and control measures configured in the MEIC model are summarized in a series of papers (Zhang et al., 2009; Zheng et al., 2014, 2018; Liu et al., 2015; Li et al., 2017, 2019).

In the MEIC model, a detailed four-level source classification system, representing sector, fuel/product, technology/solvent type, and end-of-pipe pollutant abatement facilities, was established by including over 700 emitting sources for each province. All anthropogenic sources, including power plants, industrial sources, volatile chemical products, fossil fuel burning in residential stoves, transportation were all considered.

Power plants are treated as point sources in the MEIC model. The VOC emissions were derived from the China coal-fired Power Plant Emissions Database (CPED, (Liu et al., 2015)), which is developed based on information of each unit on fuel type, fuel quality, combustion technology, etc.

Volatile chemical products are comprised of solvent use applied for architecture, vehicles, wood, and other industrial purposes, glue use, printing, pesticide use, and domestic solvent use. The market share of waterborne and solvent-based paint is further taken into account for each source category. For the on-road transportation sector, the improved emissions developed by

95 Zheng et al. (2014) were integrated into the framework of MEIC, which estimated the vehicle

96 population and emission factors at a county level. Both the VOC emissions in running mode and

97 evaporation were considered. Emission standards covering pre-Euro I and Euro I to Euro V in

98 Beijing were applied for each vehicle type (Zheng et al., 2018; Li et al., 2019). Regarding

99 oxygenated volatile organic compounds (OVOCs), the emission factors for on-road vehicles

100 were corrected, as current emission factors are only for non-methane hydrocarbons (NMHC).

101 Correction ratios of 1.32, 1.08, 1.10, and 1.06 were applied for heavy-duty and light-duty diesel

102 vehicles, and heavy-duty and light-duty gasoline vehicles, respectively, to the original values to

103 comply with the follow-up speciation for the total VOC, following the method of Li et al. (2014,

104 2019).

105

106 *Speciation of VOC emissions*

107 Emissions by individual chemical species were developed based on the

108 profile-assignment approach (Li et al., 2014, 2019). First, a "composite" profile database for

109 China was established by integrating the local profiles and supplementing it with the SPECIATE

110 v4.5 database for absent sources ((Simon et al., 2010), available at:

111 https://www.epa.gov/air-emissions-modeling/speciate-version-45-through-40). The detailed

112 procedure for developing the composite profile database is illustrated in Li et al. (2014). In brief,

113 for sources where there are significant differences in technology or legislation between China

114 and western countries, only local profiles are used; otherwise, all candidate profiles are included

115 for further compilation in the composite profile database. Local profiles covering most of the

116 important sources were gathered and reviewed, including biofuel combustion, coal combustion,

asphalt production, oil production, refinery, paint use, gasoline evaporation, gasoline vehicle exhaust, diesel vehicles, and so on, as detailed illustrated in Li et al. (2019).

Then, profiles for all combustion-related sources, including fossil fuel combustion in power plants, industry, residential, and transportation sectors were reviewed, and incomplete profiles that were absent from the OVOC fractions were corrected by appending the component of "OVOC" with fractions derived from the "complete" profiles for the same source. After OVOC correction, all "candidate" profiles were averaged by species to establish the composite profile database. Finally, the composite profile to each source was assigned by setting up the source linkage between the profile database and the inventory. Emissions by individual chemical species for each source were then further developed.

Section S3 London/United Kingdom Emission Inventory

Anthropogenic VOC emissions

The National Atmospheric Emissions Inventory (NAEI) estimates UK emissions of VOCs from anthropogenic sources following methods in the EMEP/EEA Emissions Inventory Guidebook (EMEP/EEA, 2016) for submission under the revised EU Directive 2016/2284/EU on National Emissions Ceilings (NECD), available at: https://eur-lex.europa.eu/legal-content/EN/TXT/PDF/?uri=CELEX:32016L2284&from=EN, and the United Nations Economic Commission for Europe (UNECE) Convention on Long-Range Transboundary Air Pollution (CLRTAP), available at: http://www.ceip.at/ms/ceip_home1/ceip_home/reporting_instructions/reporting_programme/. The NECD and CLRTAP define those VOC sources to be included and excluded from the

139 national inventory (for example, emissions of NMVOCs from biogenic sources are not included).

140 The Guidebook provides estimation methodologies and default emission factors for each source

141 category, although countries can use country-specific emission factors where these are deemed

142 relevant. The NAEI currently covers organic emissions from around 400 individual source

143 categories, with a large contribution from a diverse range of industrial processes and solvents,

144 but with very few individually dominant sources. The inventory then speciates emissions into

145 ~650 individual compounds, or groups of compounds. Groupings of organics, for example,

146 expressed as 'sum of all C14 compounds,' make up a substantial fraction of IVOC emissions,

147 rather than being reported as individual compounds.

148   Emissions from the use of solvents and other volatile chemicals in industry and in

149 consumer products, fuel production and distribution, food and drink manufacture and other

150 non-combustion industrial processes accounted for 72% of all UK NMVOC emissions in 2017,

151 according to the NAEI. Both the solvent and industrial process sectors cover a diverse range of

152 emission source categories: the NAEI identifies 136 separate categories across the two sectors

153   For the road transport sector, the NAEI reports exhaust emissions of NMVOCs and its

154 emissions from evaporative losses of fuel vapor from petrol vehicles. Emissions from re-fueling

155 at filling stations are reported separately under the fugitive emissions from the fuel distribution

156 sector. The method used for road transport in the NAEI follows the method in the European

157 COPERT 5 model and described in the EMEP/EEA Emissions Inventory Guidebook. The

158 method uses average speed-related emission factors for hot exhaust emissions of total

159 hydrocarbons for detailed vehicle categories (vehicle type, weight and/or engine size) and Euro

160 standards for petrol cars, diesel cars, petrol and diesel light goods vehicles, rigid and articulated

HGVs, buses and coaches, and mopeds and motorcycles, and combines these with detailed traffic and fleet activity data derived from information provided by DfT. Separate estimates are made of methane emissions for each vehicle type and subtracted from the THC emissions to derive the NMVOC emissions.

Evaporative emissions from vehicles are estimated in the NAEI, using the Guidebook method for three different processes: diurnal losses, hot soak, and running losses. Emissions are dependent on ambient temperature and fuel vapor pressure and different factors are provided for vehicles with and without carbon canisters for evaporative emission controls. All vehicles from Euro 1 onwards are fitted with these devices; so, evaporative emission have been decreasing from the early 1990s with the penetration of these vehicles in the fleet. The method also takes into account the reduction in Reid Vapour Petrol of petrol sold in the UK since 2000, as required for compliance with the EU Fuel Quality Directive 98/70/EC, amended by Directive 2009/30/EC.

Speciation of VOC emissions

The NAEI is considered to adequately reflect annual real world emissions of BTEX (see, for example, eddy covariance flux comparisons in London by Langford et al. (2010) and Vaughn et al. (2017)); so, those values are taken directly from the NAEI and used here. IVOCs, and particularly long chain hydrocarbons, are included in many cases in the inventory as groups, but their emissions are known to be significantly underestimated when compared against field observations. We use the observations of Dunmore et al. (2015), made in wintertime central London in 2012, as guide to uprate NAEI emissions for IVOC species based on the estimated

discrepancies between inventory and field observation reported for each carbon number above C10. This leads to some significant multipliers being applied to the inventory values, sometimes of the order 60 to 70. We assume that the same multipliers apply to all sources, since field data does not provide any means to attribute different factors to road transport IVOCs compared with IVOCs from VCP sources.

Since the NAEI represents a reporting of emissions for the purposes of compliance with international treaties, some fraction of those emissions are not released on the mainland UK. For this paper, offshore BTEX and IVOC emissions, arising for example from offshore oil and gas activity, aircraft in cruise, or shipping and emissions associated with overseas Crown Dependencies are removed from the UK total, since they play no part in determining the chemical environment of London. The annual NAEI totals are then divided equally to give a daily national emission.

S4 Ozone Sensitivity to ASOA Simulations

A potential issue in the attribution of premature mortality to AOSA is that reducing emissions that lead to ASOA is that this may impact ozone concentrations. A sensitivity analysis was conducted, where the ASOA emissions were reduced by 20% (Fig. S12). In general, there is a less than 1% reduction in total ozone concentration in the boundary layer. This is due to the fact that the most important AVOCs that contribute to ozone formation are light alkenes (e.g., ethylene and propylene, Fig. 5), which are not ASOA precursors. Though the reaction rate constant of the ASOA precursors is generally high (Table S11), the concentration of the precursors is low and they thus account for a low percentage of the total ozone production

205 potential (Table S5 through Table S9). For example, the measured OH reactivity (Sect. 3) for two

206 different urban regions was between 15 to 25 s^{-1} (Griffith et al., 2016; Whalley et al., 2016)

207 while the OH reactivity for the ASOA precursors for the same region was between 2 to 4 s^{-1}. The

208 small contribution to the OH reactivity is in line to the minimal impact to the ozone

209 concentration observed in Fig. S12.

Supporting Information Tables

Table S1. List of instruments whose observations are used in this study. In some cases $\Delta SOA/\Delta CO$ (Table S4), SOA versus O_x slope (Table S4), or VOC emission ratios (Table S5 through Table S8) had already been reported, and, in those cases, we use the previous literature reports in our analyses.

Location	SOA	O_x	HCHO	PAN	VOCs	CO
Houston, TX, USA (2000)	Q-AMS[a]	CL & UV Absorpion[b]	DOAS[c]	GC-ECD[d]	GC-FID, GC-MS[e]	Infrared Absortion[f]
Mexico City, Mexico (2006)	HR-ToF-AMS[g]	CL[h]	TDLAS[i]	CIMS[j]	WAS[k]	UV RF[l]
Los Angeles, CA, USA (2010)	HR-ToF-AMS[g]	CL & UV Absorption[m]	Average of DOAS[c] & Hantzsch Reaction[n]	GC-ECD[d]	GC-MS[o]	UV RF[l]
Beijing, China (2011)	HR-ToF-AMS[g]	CL & UV Absorption[p]	PTR-MS[q]	GC-ECD[r]	GC-FID[s]	IR Absorption[p]
London, UK (2012)	C-ToF-AMS[t]	CL & UV Absorption[u]	Hantzsch Reaction[n]	GC-ECD[v]	GC-FID & GC×GC-FID[w]	UV RF[l]
Houston, TX, USA (2013)	HR-ToF-AMS[g]	CL[x]	Average of LIF[y] & CAMS[z]	CIMS[j]	WAS[k]	DACOM[aa]
Seoul, South Korea (2016)	HR-ToF-AMS[g]	CL[h]	CAMS[z]	CIMS[j]	WAS[k]	DACOM[aa]

[a]Quadrupole Aerosol Mass Spectrometer (Q-AMS) (Jayne et al., 2000)

[b]Chemiluminescence (CL) and UV Absorption (Williams et al., 1997)

[c]Differential Optical Absorption Spectrometry (DOAS) (Stutz and Platt, 1996, 1997)

[d]Gas chromatography-electron capture detector (GC-ECD) (Williams et al., 2000; Roberts et al., 2002)

[e]Gas chromatography-flame ionization detector (GC-FID) and gas chromatography mass spectrometer (Roberts et al., 2001)

[f]TECO Model 48s IR gas-filter

[g]High Resolution Time-of-Flight Aerosol Mass Spectrometer (HR-ToF-AMS) (DeCarlo et al., 2006)

[h]Chemiluminescence (CL) and UV Absorption (Weinheimer et al., 1994)

[i]Tunable diode laser absorption spectroscopic (TDLAS) measurements (Fried et al., 2003)

[j]Chemical ionization mass spectrometer (CIMS) (Huey L Tanner D Slusher D Dibb J Arimoto R Chen G Davis D Buhr M Nowak J Mauldin R Eisele F, 2004; Slusher et al., 2004; Kim et al., 2007)

[k]Whole air sample, followed by analysis with GC-FID and/or GC-MS (Blake et al., 2003)

[l]UV Resonance Fluorescence (RF) (Gerbig et al., 1999)

233 [m]Chemiluminescence (CL) and UV Absorption (Hayes et al., 2013)
234 [n]Hantzsch reaction (Cárdenas et al., 2000)
235 [o]Gas chromatograph mass spectrometer (Gilman et al., 2010)
236 [p]Chemiluminescence (CL), UV Absorption, and IR Absorption (Hu et al., 2016)
237 [q]Proton transfer reaction mass spectrometer (PTR-MS) (Warneke et al., 2011)
238 [r]Gas chromatography electron capture detector (GC-ECD) (Zhang et al., 2017)
239 [s]Gas chromatography flame ionization detector (GC-FID) (Wang et al., 2014)
240 [t]Compact Time-of-Flight Aerosol Mass Spectrometer (C-ToF-AMS) (Drewnick et al., 2005)
241 [u]Chemiluminescence (CL) and UV Absorption (Whalley et al., 2016)
242 [v]Gas chromatography electron capture detector (GC-ECD) (Whalley et al., 2016)
243 [w]Gas chromatography flame ionization detector (GC-FID) (Dunmore et al., 2015)
244 [x]Chemiluminescence (CL) (Ryerson et al., 1999; Pollack et al., 2010)
245 [y]Laser induced fluorescence (LIF) (Cazorla et al., 2015)
246 [z]Compact Atmospheric Multi-species Spectrometer (CAMS) difference frequency absorption
247 spectrometer (Weibring et al., 2010)
248 [aa]Tunable diode laser absorption spectroscopy (Sachse et al., 1987)

Table S2. Concentrations of PM$_1$ components shown in Fig. 1. References for the measurements can be found in Table 1.

Dataset Location	Average Concentration (μg sm^{-3}) of submicron aerosol under standard temperature and pressure				
	SOA	HOA	SO$_4$	NO$_3$	NH$_4$
Houston, TX, USA (2000)	2.7	0.7	4.9	0.4	1.5
Northeast USA (2002)	4.9	0.5	2.0	0.3	0.7
Tokyo, Japan (2004)	6.0	1.5	4.4	0.9	4.0
Mexico City, Mexico (2006)	11.2	4.8	1.9	6.0	2.5
Paris, France (2009)	1.9	1.1	1.2	0.5	0.6
Los Angeles, CA, USA (2010)	5.0	2.0	2.9	3.6	2.1
Changdao Island, China (2011)	9.4	4.4	8.3	12.2	6.5
Beijing, China (2011)	17.1	8.9	22.0	16.8	13.7
London, UK (2012)	2.7	1.6	1.4	2.7	1.3
Houston, TX, USA (2013)	3.7	0.0	2.7	0.1	0.6
New York City, NY, USA (2015)	0.8	0.7	1.2	1.4	0.4
Seoul, South Korea (2016)	11.9	1.3	5.0	7.9	4.4

253 **Table S3.** Table summarizing the results of recent GEOS-Chem performance evaluations for
254 modeling BSOA.

Study	Observed Data	Species	Details
Fisher et al. (2016)[a]	SEAC[4]RS, below 1 km (spatial pattern), below 500 m (bias)	Isoprene	Spatial patterns well captured, and biases are +34% for isoprene and +3% for monoterpenes
		Monoterpene	
		Organic Nitrates from Isoprene	Spatial patterns well captured, and biases are -0.6% for first- and -35% for second-generation isoprene nitrates
	SEAC[4]RS, 0 - 4 km vertical profiles	Isoprene	Agreed well but GEOS-Chem somewhat overestimated observed concentrations near 1km
		Monoterpene	
		HCHO	
		Organic Nitrates from Isoprene	Agreed within measurement uncertainties
	SOAS, at the surface	Isoprene	Underestimated isoprene and monoterpenes (-28% and -54%), but overestimated first- and second- generation isoprene nitrates (+85% and +43%)
		Monoterpene	
		HCHO	
		Organic Nitrates from Isoprene	
Travis et al. (2016)	SEAC[4]RS, 0 - 12 km	First Generation from Isoprene Nitrates	Good agreement for ISOPOOH and ISOPN, underestimation of HPALDs by a factor of two
		ISOPOOH	
		HPALDS	
Marais et al. (2016)	SOAS, at the surface	IEPOX-SOA	Good agreement for isoprene derived aerosols, mean concentrations were almost the same
		ISOPOOH-SOA	
	SEAC[4]RS, below 2 km (spatial pattern)	IEPOX-SOA	Spatial patterns well captured

255 [a]This study decreased isoprene emissions by 15% and doubled monoterpene emissions of
256 MEGANv2.1.

Table S3 cont.

Study	Observed Data	Species	Details
Kaiser et al. (2018)[a]	SEAC⁴RS	Isoprene	All were overestimated, except for first generation isoprene nitrates
		HCHO	
		ISOPOOH	
		MVK + MACR	
		First Generation Isoprene Nitrates	
Pai et al. (2020)	15 airborne campaigns (SEAC⁴RS, GoAmazon, SENEX, OP3, etc.)	OA under biognic dominant conditions	Slight overestimation, but generally very similar in magnitude

[a]NEI NO_x emissions other than power plants decreased by 60%, soil NO_x emissions were reduced by 50% across the Midwestern US. With the decrease of NO_x emissions, ISOPOOH concentrations were increased in GEOS-Chem.

Table S4. Dilution-corrected SOA concentrations at 0.5 equivalent days and slopes of SOA versus O_x, HCHO, and PAN used in Fig. 4 and Fig. 5. References for the values can be found either in Table 1 or found in Fig. S2 through Fig. S4. Uncertainty is 1σ, and either represents propagation in uncertainty in measurements (see Sect. 2 Main Paper) for ΔSOA/ΔCO or uncertainty in slopes for SOA versus the three photochemical species.

Dataset Location	ΔSOA/ΔCO at 0.5 eq. days	SOA vs. O_x Slopes	SOA vs. HCHO Slopes	SOA vs. PAN Slopes
Houston, TX, USA (2000)		0.04±0.01[a]	0.32±0.08	1.41±0.46
Northeast USA (2002)	16±3[b] 48±9[c]			
Mexico City, Mexico (2003)		0.14±0.01[a]		
Tokyo, Japan (2004)		0.19±0.01[a]		
Mexico City, Mexico (2006)	58±10	0.16±0.01	1.60±0.06	5.60±0.30
Paris, France (2009)		0.14±0.01[a]		
Pasadena, CA, USA (2010)	59±11	0.16±0.01	1.93±0.02	5.41±0.12
Changdao Island, China (2011)	23±4			
Beijing, China (2011)	31±6	0.21±0.01	3.90±0.15	7.42±0.46
London, UK (2012)	54±10	0.13±0.01	0.36±0.02	3.37±0.41
Houston, TX, USA (2013)		0.16±0.01	1.52±0.13	6.92±0.58
New York City, NY, USA (2015)	33±6			
Seoul, South Korea (2016)	107±19	0.29±0.02	3.73±0.26	10.13±0.52

[a]Missing reported uncertainty; therefore, assuming ±0.01, as that is typical for other campaigns
[b]From de Gouw et al. (2005). [c]From Kleinman et al. (2007).

Table S5. Emission ratios of BTEX aromatics used in this study. If no reference is listed, then the emission ratio was calculated using Eq. 3.

Dataset Location	Emission Ratios (ppbv aromatic/ppmv CO)					References
	Benzene	Toluene	Ethylbenzene	m+p-xylene	o-xylene	
Houston, TX, USA (2000)	2.6	3.5	0.6	2.8	0.8	
NE USA, Ship (2002)	0.9	2.0	0.2	0.6	0.3	Baker et al. (2008)
NE USA, Aircraft (2002)	0.8	2.9	0.4	1.2	0.5	Warneke et al. (2007)
Mexico City, Mexico (2006)	0.9	7.5	0.9	1.1	0.4	Apel et al. (2010)
Los Angeles, CA, USA (2010)	1.3	3.4	0.6	2.1	0.8	de Gouw et al. (2017)
Changdao Island, China (2011)	2.3	1.9	0.5	1.3	0.4	Yuan et al. (2013)
Beijing, China (2011)	1.2	2.4	1.0	1.6	0.6	Wang et al. (2014)
London, UK (2012)	1.8	6.3	1.2	2.2	1.1	
Houston, TX, USA (2013)	2.3	3.0	0.6	3.9	1.2	
New York City, NY, USA (2015)	0.8	2.9	0.4	1.2	0.5	Warneke et al. (2007)[a]
Seoul, South Korea (2016)	1.1	13.1	2.4	3.3	2.3	

[a]Using the emissions from Warneke et al. (2007) instead of Schroder et al. (2018) as Schroder et al. found significant uncertainty in the emissions calculated from observations.

272 **Table S6**. Emission ratios of alkanes used in this study. If no reference is listed, then the
273 emission ratio was calculated using Eq. 3.

Dataset Location	Emission Ratios (ppbv alkane/ppmv CO)							References
	Ethane	Propane	n-Butane	i-Butane	n-Pentane	i-Pentane	n-Hexane	
Houston, TX, USA (2000)	40.9	24.3	9.0	14.7	3.1	10.0	3.1	
NE USA, Ship (2002)	8.3	2.3	1.8	1.3	1.0	2.8	0.9	Baker et al. (2008)
NE USA, Aircraft (2002)	9.9	9.0	2.4	1.3	2.0	5.4	0.6	Warneke et al. (2007)
Mexico City, Mexico (2006)	7.4	41.5	15.1	4.8	2.1	2.7	1.5	Apel et al. (2010)
Los Angeles, CA, USA (2010)	16.5	13.4	5.0	3.2	3.4	8.7	1.4	de Gouw et al. (2017)
Changdao Island, China (2011)	7.7	4.5	2.5	1.2	1.0	1.5	0.5	Yuan et al. (2013)
Beijing, China (2011)	4.3	3.9	2.5	2.5	1.2	2.0	0.6	Wang et al. (2014)
London, UK (2012)	33.0	17.8	17.3	8.4	4.6	11.3	1.3	
Houston, TX, USA (2013)	86.5	37.3	14.6	10.6	7.0	10.5	3.0	
Seoul, South Korea (2016)	16.1	0.4	6.0	3.4	3.1	3.7	1.7	

274

Table S7. Emission ratios of alkenes used in this study. If no reference is listed, then the emission ratio was calculated using Eq. 3.

Dataset Location	Emission Ratios (ppbv alkene/ppmv CO)		References
	Ethene	Propene	
Houston, TX, USA (2000)	24.4	28.4	
NE USA, Ship (2002)	4.4	1.1	Baker et al. (2008)
NE USA, Aircraft (2002)	4.9	1.4	Warneke et al. (2007)
Mexico City, Mexico (2006)	8.4	2.6	Apel et al. (2010)
Los Angeles, CA, USA (2010)	11.2	4.1	de Gouw et al. (2017)
Changdao Island, China (2011)	5.3	1.4	Yuan et al. (2013)
Beijing, China (2011)	4.4	1.4	Wang et al. (2014)
London, UK ()2012)	10.3	6.2	
Houston, TX, USA (2013)	12.0	15.8	
Seoul, South Korea (2016)	5.4	2.1	

278 **Table S8**. Emission ratios of non-BTEX aromatics used in this study. If no reference is listed,
279 then the emission ratio was calculated using Eq. 3.

Dataset Location	Emission Ratios (ppbv aromatic/ppmv CO)			References
	Trimethylbenzenes	Ethyltoluenes	Propylbenzene	
NE USA, Aircraft (2002)	0.71	0.58	0.14	Warneke et al. (2007)
Los Angeles, CA, USA (2010)	1.47	0.56	0.13	de Gouw et al.(2017)
Beijing, China (2011)	0.57	0.41	0.09	Wang et al. (2014)
London, UK (2012)	0.49	0.23	0.58	
New York City, NY, USA (2015)	0.71	0.58	0.14	Warneke et al. (2007)

280
281
282 **Table S9**. Normalized mass concentration of primary organic aerosol (POA) measured in various
283 campaigns, used to determine SVOC emission ratios.

Dataset Location	Normalized Mass Concentration ($\mu g\ sm^{-3}$)		References
	HOA	Other POA	
NE USA (2002)	12.2	-	de Gouw et al. (2005)
Los Angeles, CA, USA (2010)	5.3	7.7	Hayes et al. (2013)
Beijing, China (2011)	6.1	9.9	Hu et al. (2016)
London, UK (2012)	17.9	14.1	Young et al. (2015)
New York City, NY, USA (2015)	5.6	14.4	Schroder et al. (2018)

284

Table S10. Sensitivity analysis of slopes and R^2 by removing one city each. All slopes are statistically similar at the 95% confidence interval.

Dataset Location	Slope (µg sm⁻³ s)	R^2
All	24.8±3.4	0.88
Without Seoul	34.0±10.5	0.64
Without NYC	24.8±3.8	0.8
Without London	24.2±3.4	0.90
Without Beijing	24.2±3.5	0.89
Without Chinese Outflow	24.0±3.6	0.88
Without LA	24.2±3.3	0.90
Without Mexico City	24.2±3.4	0.90
Without NE US Aircraft	24.8±2.9	0.92
Without NE US, Boat	24.2±4.0	0.86

288 **Table S11**. Rate constants used throughout this study.

Compound	Rate Constant $(cm^3\ molec.^{-1}\ s^{-1})$	References
Alkanes		
Ethane	$6.9\times10^{-12}\times\exp(-1000/T)$	Atkinson et al. (2006)
Propane	$7.6\times10^{-12}\times\exp(-585/T)$	Atkinson et al. (2006)
n-Butane	$9.8\times10^{-12}\times\exp(-425/T)$	Atkinson et al. (2006)
i-Butane	$1.17\times10^{-17}\times T^2\times\exp(213/T)$	Atkinson and Arey (2003)
n-Pentane	$2.52\times10^{-17}\times T^2\times\exp(158/T)$	Atkinson and Arey (2003)
i-Pentane	3.6×10^{-12}	Atkinson and Arey (2003)
n-Hexane	$2.54\times10^{-14}\times T\times\exp(-112/T)$	Atkinson and Arey (2003)
Alkenes		
Ethene	$7.84\times10^{-12,a}$	Atkinson et al. (2006)
Propene	$2.86\times10^{-11,a}$	Atkinson et al. (2006)
Aromatics		
Benzene	$2.3\times10^{-12}\times\exp(-190/T)$	Atkinson et al. (2006)
Toluene	$1.8\times10^{-12}\times\exp(340/T)$	Atkinson et al. (2006)
Ethylbenzene	7×10^{-12}	Atkinson and Arey (2003)
m+p-xylene	$1.87\times10^{-11,b}$	Atkinson and Arey (2003)
o-xylene	1.36×10^{-11}	Atkinson and Arey (2003)
Trimethylbenzenes	$2.73\times10^{-12}\times\exp(730/T)$	Bohn and Zetzsch (2012)
Ethyltoluenes	1.2×10^{-11}	Atkinson and Arey (2003)
Propylbenzene	5.8×10^{-12}	Atkinson and Arey (2003)
NO_x/NO_y		
$OH + NO_2$	$1.23\times10^{-11,a}$	Mollner et al. (2010)

289 [a]Showing the rate constant at 298 K, 1013 hPa. However, for this study, we used the temperature
290 and pressure dependent formulation listed in each respective reference.
291 [b]This is the average of m-xylene and p-xylene rate constants.

292 **Table S12**. Table of GBD parameters, which is the mean of the draw values (see associated file)
293 from the IHME website:
294 http://ghdx.healthdata.org/record/global-burden-disease-study-2010-gbd-2010-ambient-air-pollut
295 ion-risk-model-1990-2010.

Parameter	IHD	Stroke	COPD	LC	ALRI
α	1.4273	1.2641	15.224	114.74	2.2023
β	0.04764	0.00722	0.00095	0.000141	0.000284
ρ	0.376	1.314	0.684	0.741	1.183
$PM_{2.5,Threshold}$	7.462	7.387	7.374	7.380	7.283

296

Table S13. Table of GEMM parameters. The GEMM parameters are from Burnett et al. (2018), with the Chinese male cohort.

Cause of Death	Age Range (years)	θ	Standard Error θ	α	μ	π
NCD + LRI	>25	0.1430	0.01807	1.6	15.5	36.8
	27.5	0.1585	0.01477	1.6	15.5	36.8
	32.5	0.1577	0.01470	1.6	15.5	36.8
	37.5	0.1570	0.01463	1.6	15.5	36.8
	42.5	0.1558	0.01450	1.6	15.5	36.8
	47.5	0.1532	0.01425	1.6	15.5	36.8
	52.5	0.1499	0.01394	1.6	15.5	36.8
	57.5	0.1462	0.01361	1.6	15.5	36.8
	62.5	0.1421	0.01325	1.6	15.5	36.8
	67.5	0.1374	0.01284	1.6	15.5	36.8
	72.5	0.1319	0.01234	1.6	15.5	36.8
	77.5	0.1253	0.01174	1.6	15.5	36.8
	85	0.1141	0.01071	1.6	15.5	36.8
IHD	>25	0.2969	0.01787	1.9	12	40.2
	27.5	0.5070	0.02458	1.9	12	40.2
	32.5	0.4762	0.02309	1.9	12	40.2
	37.5	0.4455	0.02160	1.9	12	40.2
	42.5	0.4148	0.02011	1.9	12	40.2
	47.5	0.3841	0.01862	1.9	12	40.2
	52.5	0.3533	0.01713	1.9	12	40.2
	57.5	0.3226	0.01564	1.9	12	40.2
	62.5	0.2919	0.01415	1.9	12	40.2

Table 13 cont.

Cause of Death	Age Range (years)	θ	Standard Error θ	α	μ	π
IHD	67.5	0.2612	0.01266	1.9	12	40.2
	72.5	0.2304	0.01117	1.9	12	40.2
	77.5	0.1997	0.00968	1.9	12	40.2
	85	0.1536	0.00745	1.9	12	40.2
Stroke	>25	0.2720	0.07697	6.2	16.7	23.7
	27.5	0.4513	0.11919	6.2	16.7	23.7
	32.5	0.4240	0.11197	6.2	16.7	23.7
	37.5	0.3966	0.10475	6.2	16.7	23.7
	42.5	0.3693	0.09752	6.2	16.7	23.7
	47.5	0.3419	0.09030	6.2	16.7	23.7
	52.5	0.3146	0.08307	6.2	16.7	23.7
	57.5	0.2872	0.07585	6.2	16.7	23.7
	62.5	0.2598	0.06863	6.2	16.7	23.7
	67.5	0.2325	0.06190	6.2	16.7	23.7
	72.5	0.2051	0.05418	6.2	16.7	23.7
	77.5	0.1778	0.04695	6.2	16.7	23.7
	85	0.1368	0.03611	6.2	16.7	23.7
COPD	>25	0.2510	0.06762	6.5	2.5	3.2
Lung Cancer	>25	0.2942	0.06147	6.2	9.3	29.8
LRI	>25	0.4468	0.11735	6.4	5.7	8.4

Table S14. Calculated premature mortality from PM with all aerosol (base mortality) and removing ASOA, using the IER method.

Location[a]	Base Mortality	Mortality reduced due to removing ASOA	Percent mortality reduced due to removing ASOA
North America	43,408	18,479	43%
Central America	11,808	3,395	29%
South America	31,214	10,100	32%
Africa	258,294	14,869	6%
Western Europe	305,754	31,880	10%
Eastern Europe	195,749	16,003	8%
South Asia	938,967	75,085	8%
Southeastern Asia	135,433	31,886	24%
East Asia	1,315,720	122,190	9%
Oceania	95	27	28%
Rest of the World	72,385	13,337	18%
Total	3,308,957	337,224	10%

[a]Locations defined by:
http://themasites.pbl.nl/tridion/en/themasites/_disabled_image/background/regions/index-2.html

306 **Table S15**. Calculated premature mortality from PM with all aerosol (base mortality) and
307 removing ASOA, using the GEMM method.

Location[a]	Base Mortality	Mortality reduced due to removing ASOA	Percent mortality reduced due to removing ASOA
North America	178,793	24,892	14%
Central America	58,516	7,298	12%
South America	145,395	22,372	15%
Africa	765,946	34,528	5%
Western Europe	768,991	50,427	7%
Eastern Europe	465,341	25,552	5%
South Asia	2,285,903	166,228	7%
Southeastern Asia	347,191	50,802	15%
East Asia	2,487,349	220,264	9%
Oceania	3,375	428	13%
Rest of the World	269,769	35,051	13%
Total	7,776,570	638,219	8%

308 [a]Locations defined by:
309 http://themasites.pbl.nl/tridion/en/themasites/_disabled_image/background/regions/index-2.html

Table S16. List of total final consumption, in millions of tonnes of oil equivalent, of oil products and oil, for each organization. Total final consumption includes imports, and does not include exports (IEA, 2019).

Organization	Industry	Transportation	Non-Energy
World	307	2533	645
OECD	89	1147	326
Africa	18.4	115.4	7.9
Non-OECD	28.3	135	20
Middle East	33.5	126.3	47.5
Non-OECD Europe and Eurasia	35	101	53

Supplemental figures for this study

315

316

317

Figure showing scatter plot with:
Slope = 1.48(±0.05)
Intercept = −0.23(±0.10)
R^2 = 0.82

Axes: HCHO (ppbv, DOAS) vs HCHO (ppbv, Hantzsch)
Legend: Slope, 1:1 Line
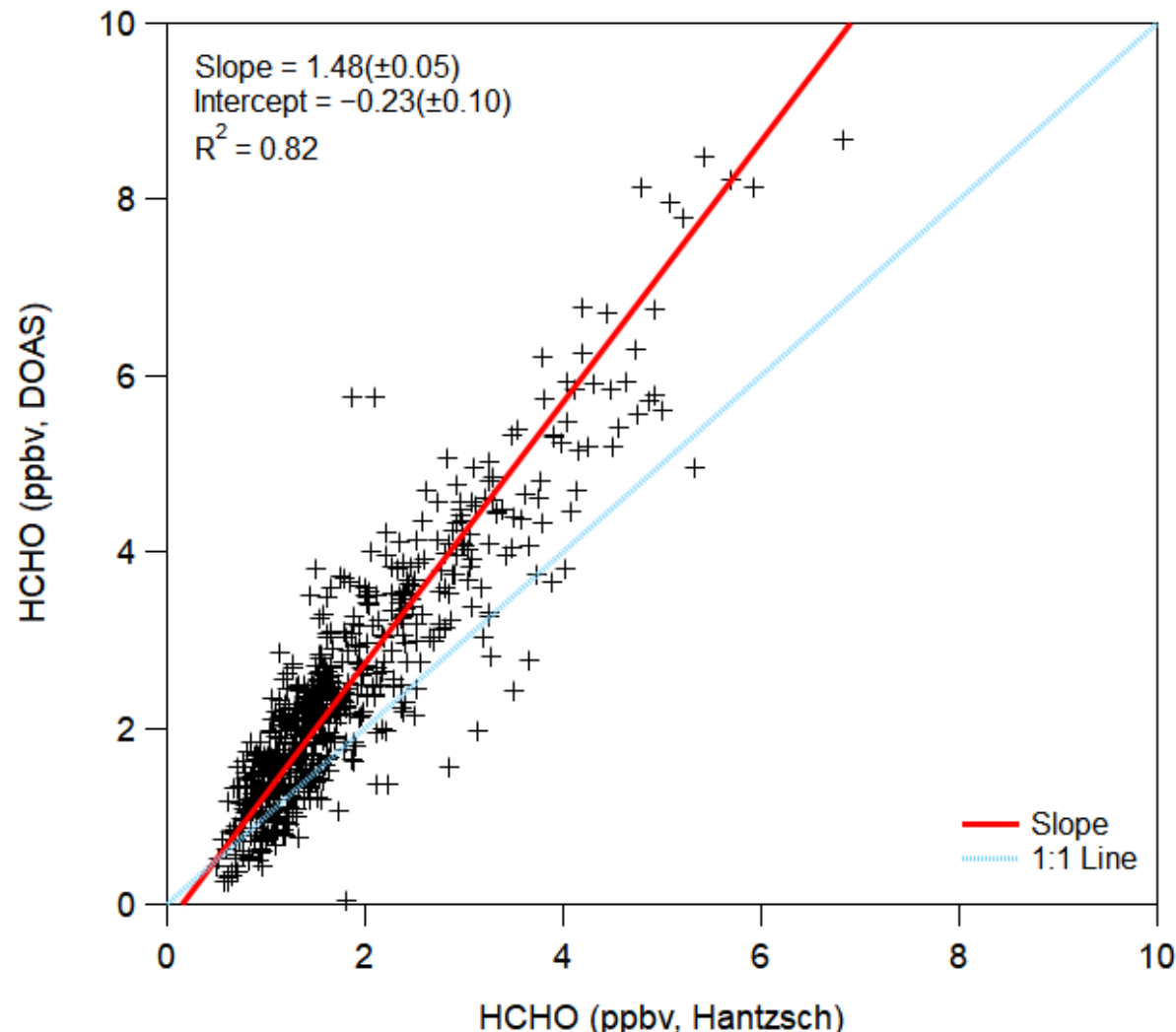
318 **Figure S1**. Comparison of HCHO measured by the DOAS (Stutz and Platt, 1996, 1997) and
319 Hantzsch reaction (Cárdenas et al., 2000) methods during the CalNex 2010 study in Pasadena,
320 CA, ground site (Ryerson et al., 2013).
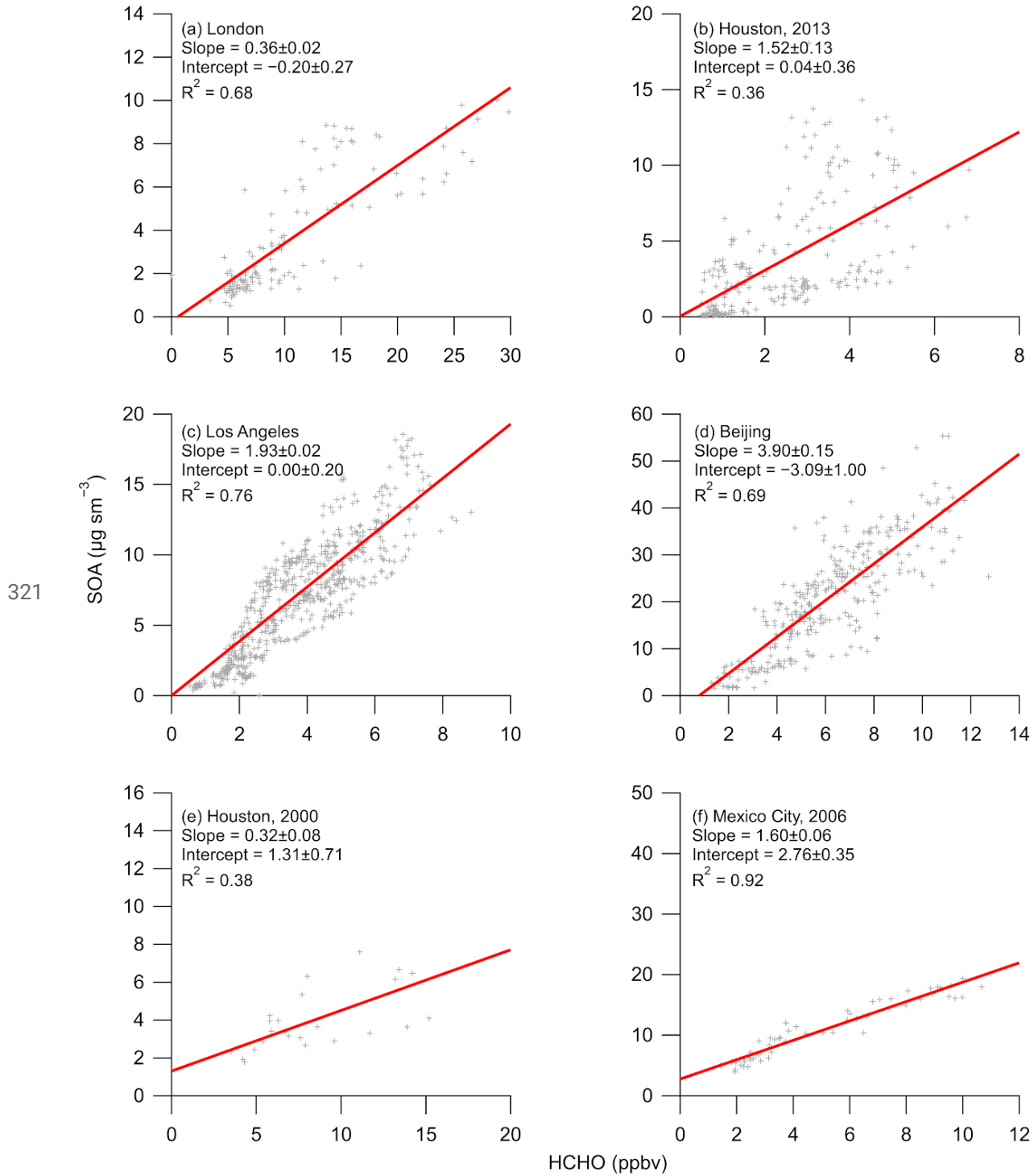
Figure S2. Regression plot of SOA versus HCHO from different campaigns around the world that have not been previously published. Note, for (c), HCHO is 1.24×Hantzsch HCHO, to account for the differences between the two HCHO measurements during CalNex. Note, for (a), SOA is 0.5×OA, estimated from Young et al. (2015), and for (f), SOA is 0.8×OA, estimated from DeCarlo et al. (2010).
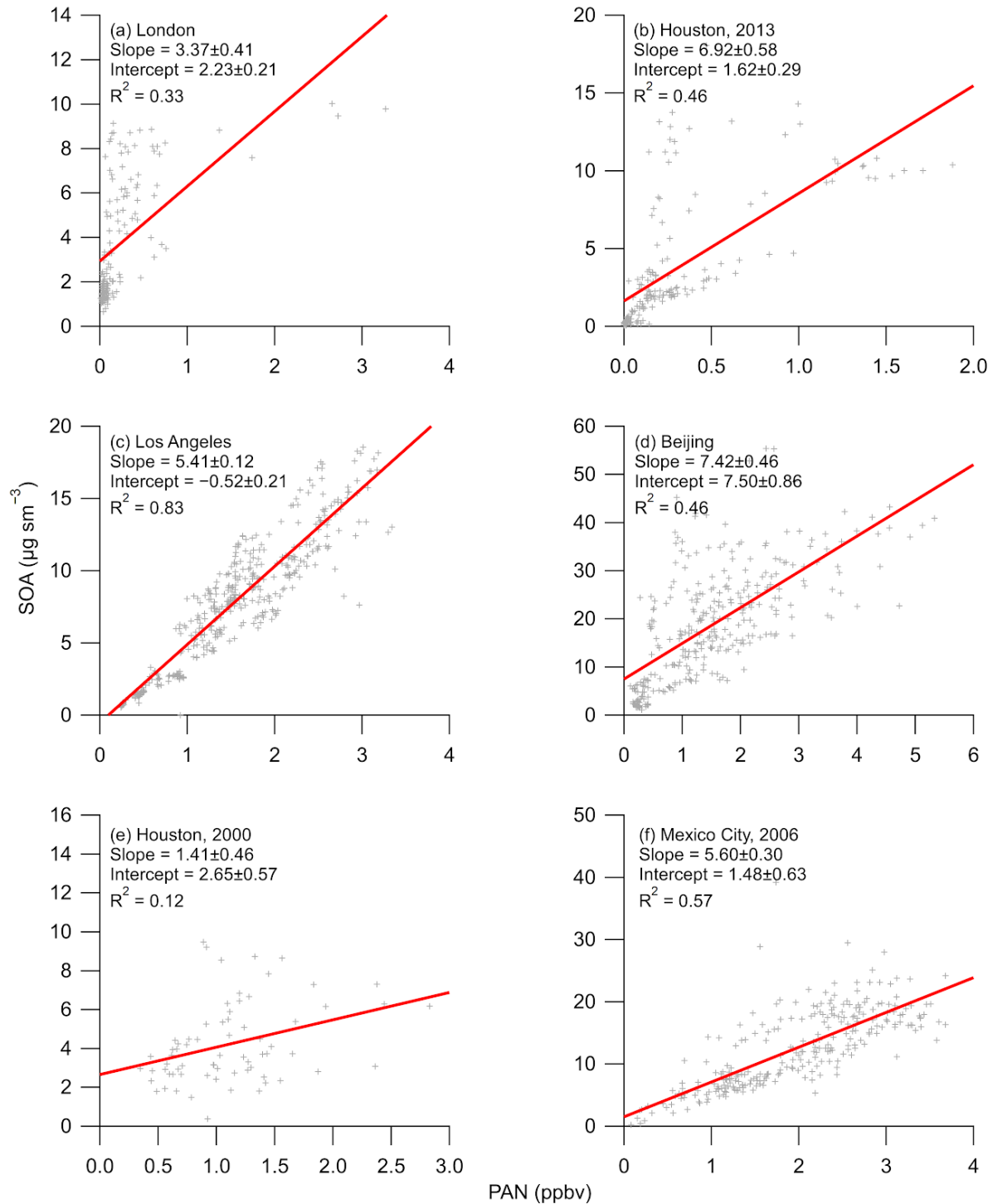
Figure S3. Regression plot of SOA versus PAN from different campaigns around the world that have not been previously published. Note, for (a), SOA is 0.5×OA, estimated from Young et al. (2015), and for (f), SOA is 0.8×OA, estimated from DeCarlo et al. (2010).

332

Figure S4 plot (a) London:
Slope = 0.13±0.01
Intercept = −2.71±0.37
$R^2 = 0.67$

Figure S4 plot (b) Houston, 2013:
Slope = 0.16±0.01
Intercept = −3.77±0.36
$R^2 = 0.72$

SOA ($\mu g\ sm^{-3}$)

O_x (ppbv)

333
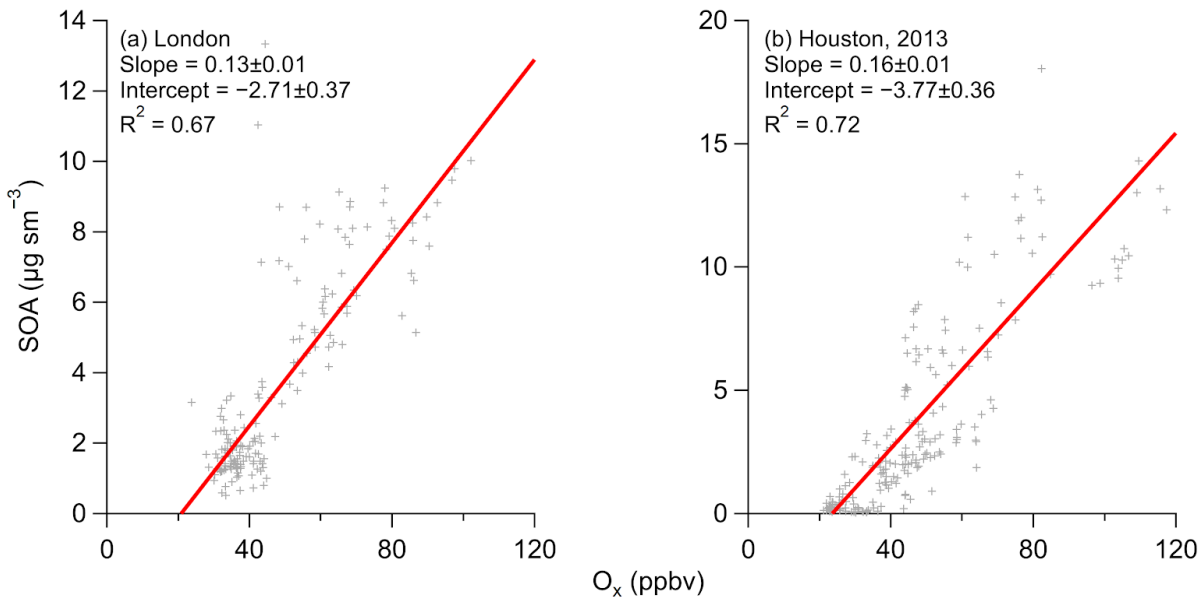
Figure S4. Regression plot of SOA versus Ox from different campaigns around the world that have not been previously published. Note, for (a), SOA is 0.5×OA, estimated from Young et al. (2015).
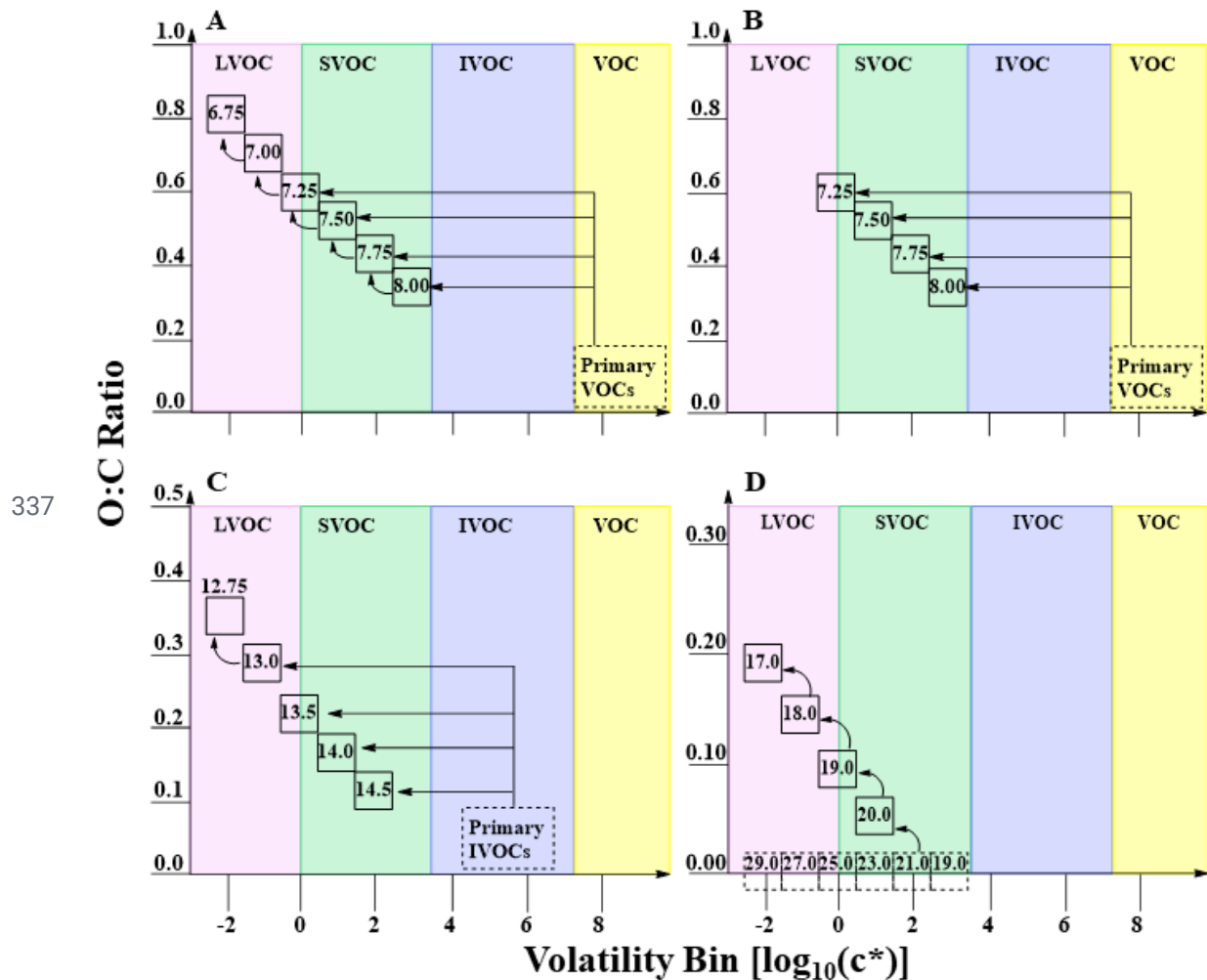
Figure S5. 2-D VBS space defined by oxygen to carbon (O:C) ratio and saturation concentration $[\log_{10}(c^*)]$ for different oxidation mechanisms and primary sources of OA precursors. Dashed boxes represent primary emissions, while the full boxes represent the secondary oxidation products. (A) and (B) represent different parameterizations for treating traditional anthropogenic and biogenic sources of SOA. Both parameterizations depict the oxidation of an 8-carbon precursor VOC. (A) represents the TSI, or aging, parameterization; (B) represents the MA, or wall-loss corrected, parameterization. (C) Represents the initial oxidation and aging pathway of P-IVOCs following the ZHAO parameterization. It should be noted that the carbon number corresponds to first generation aging and subsequent oxidation results in a 0.25 reduction in carbon number. (D) Represents the decadal aging of SVOCs by hydroxyl radicals. In (D), the full aging pathway of only the C21 species is depicted as an example, though all primary species are allowed to age until the $\log_{10}(c^*) = -2$ bin. All emitted P-SVOC species undergo the same decadal aging scheme which begins from the saturation concentration bin of the emitted species.
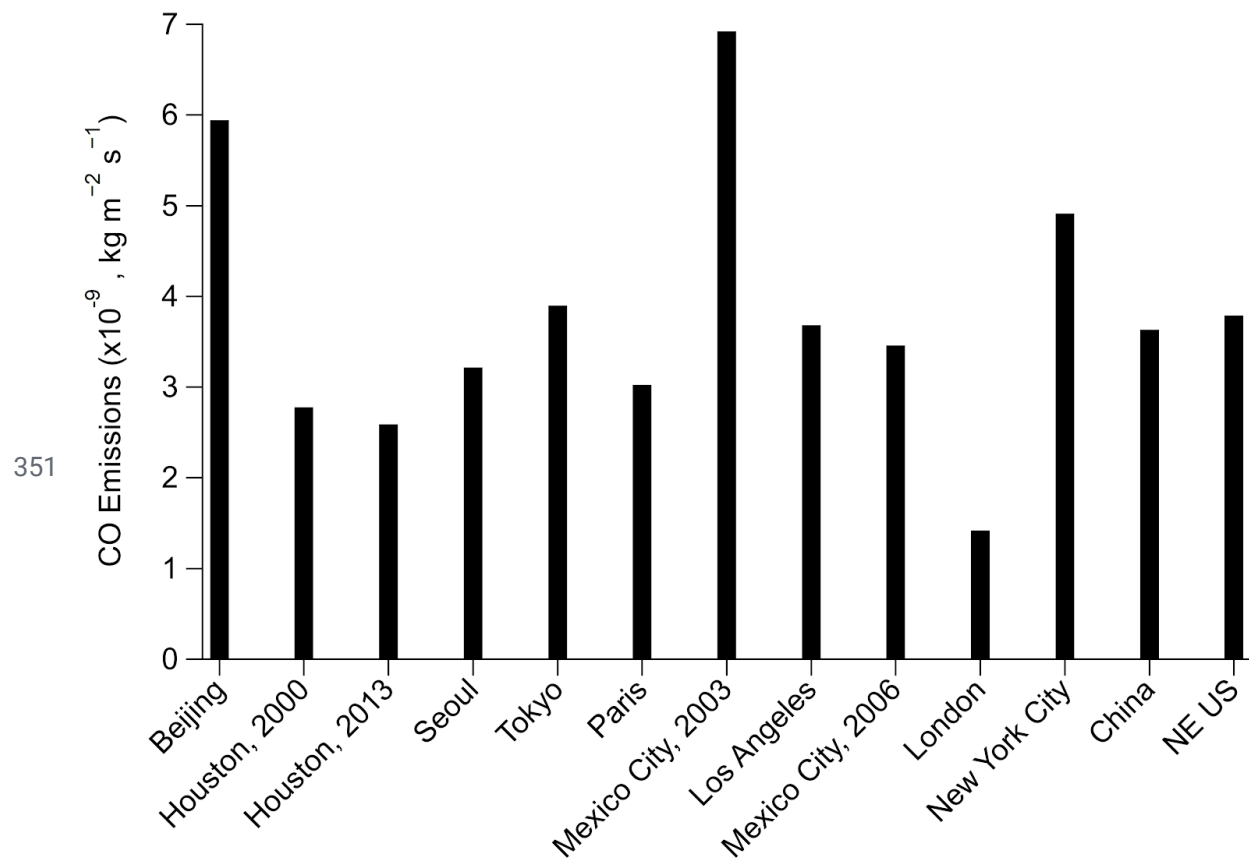
Figure S6. CO emissions for the cities investigated here from HTAP (Janssens-Maenhout et al., 2015).
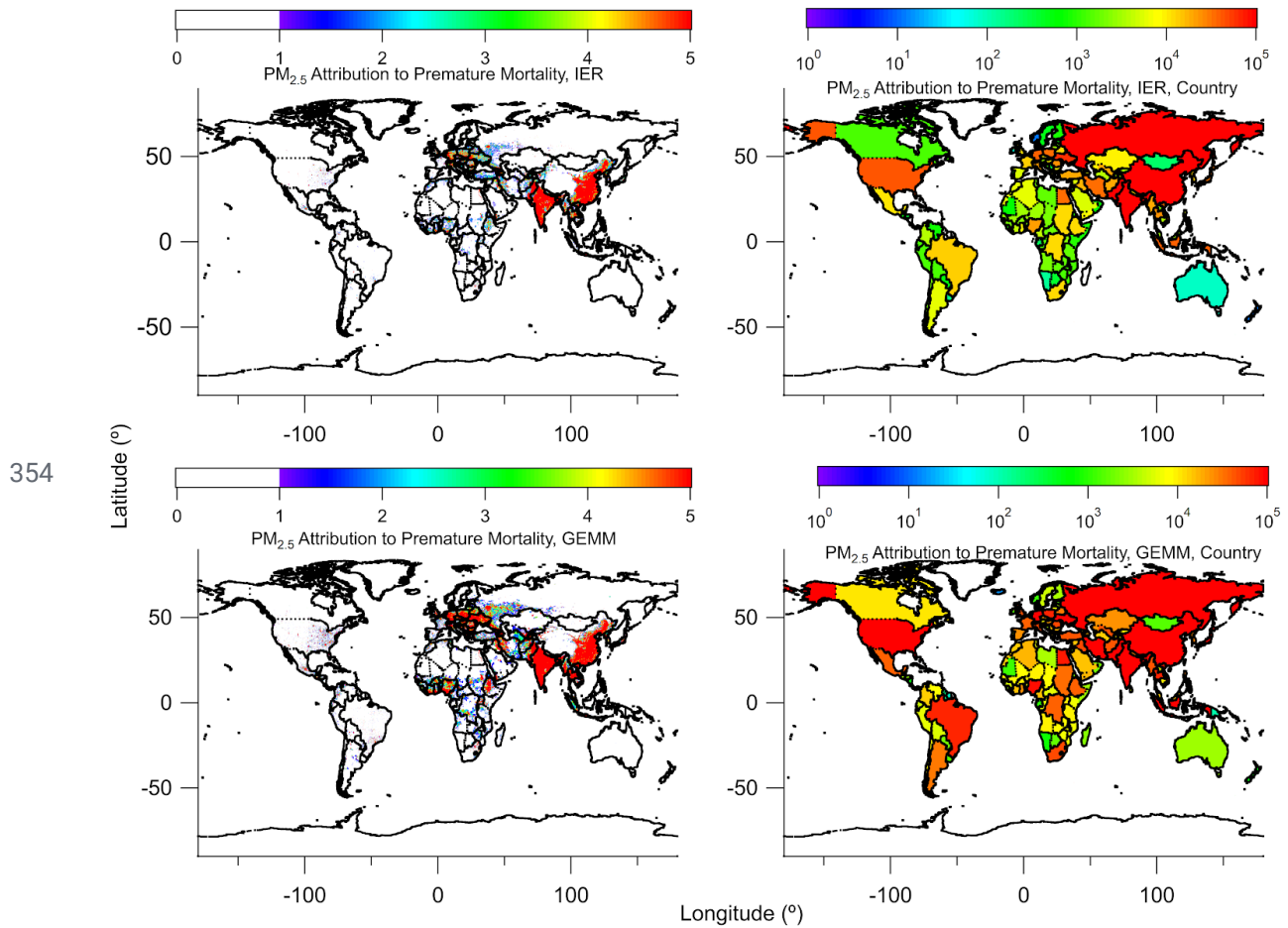
**Figure S7**. (top) Total deaths associated to PM$_{2.5}$ (left) per 10×10 km^2 area and (right) summed up for each country, using the Integrated Exposure-Response (IER) method (Burnett et al., 2014). These values are derived from satellite. (bottom) Same as above, but using the Global Exposure Mortality Model (GEMM) (Burnett et al., 2018) for PM$_{2.5}$ per 10×10 km^2 area (left) and summed up for each country (right). Premature mortality was determined with PM$_{2.5}$ derived by the methods described in van Donkelaar (2016), which includes satellite and ground-based observations of aerosol.
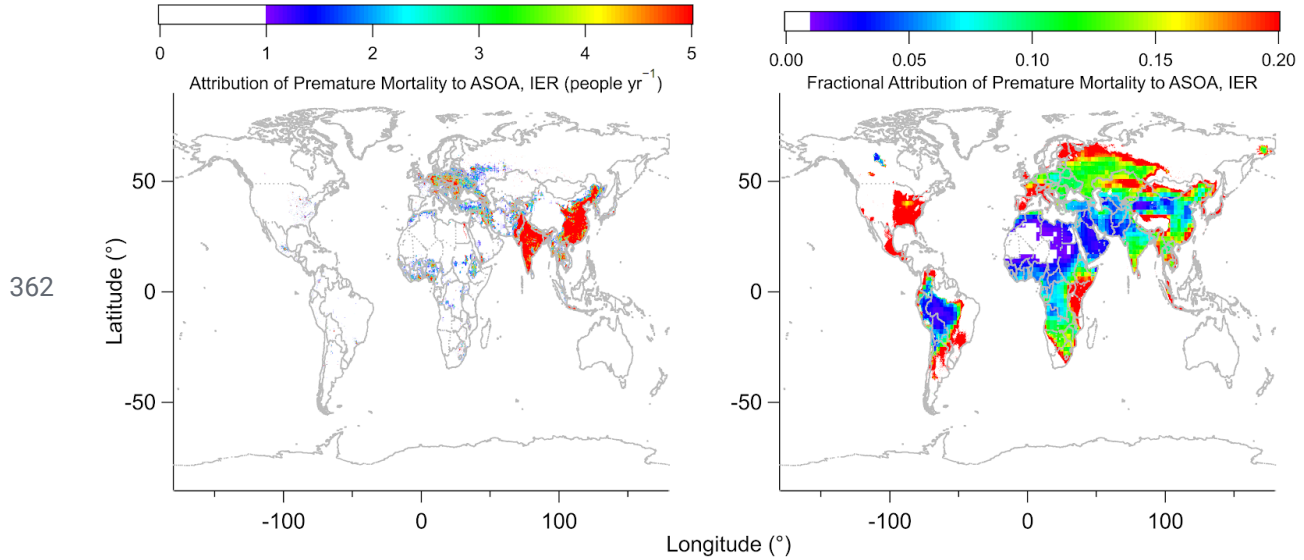
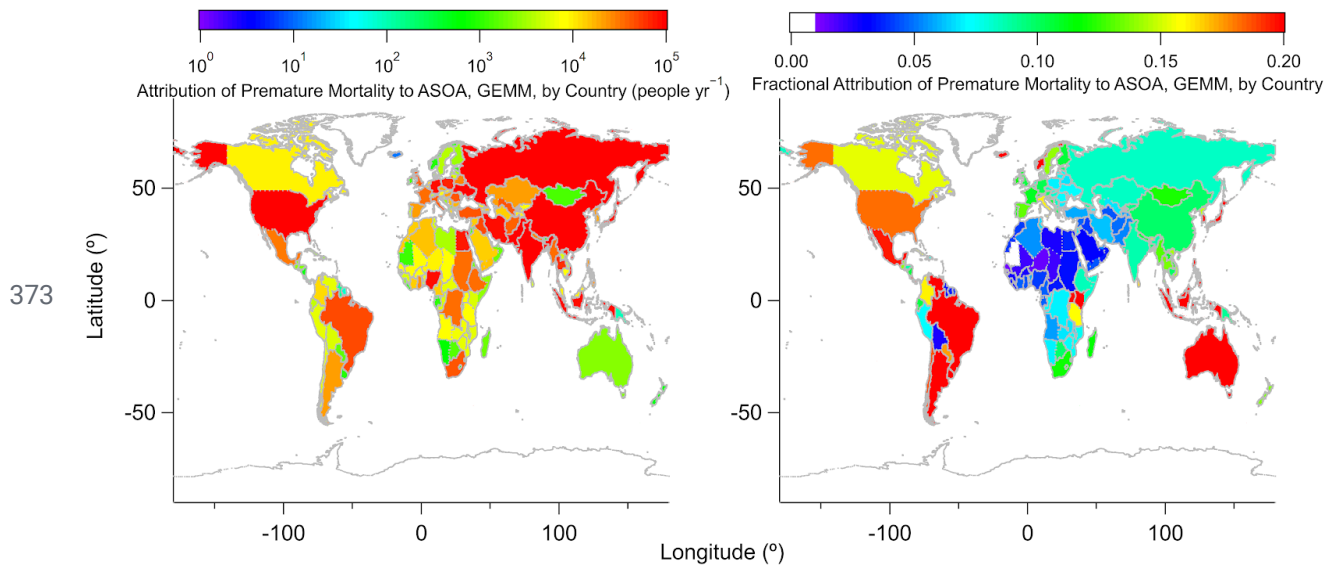**Figure S8**. Same as Fig. 8, where top are the results per 10×10 km^2 area for the attribution of premature mortality to ASOA (people yr^{-1}, left) and fractional attribution of premature mortality to ASOA for one year (right) by the IER method. See Fig. 8 for per country comparison.
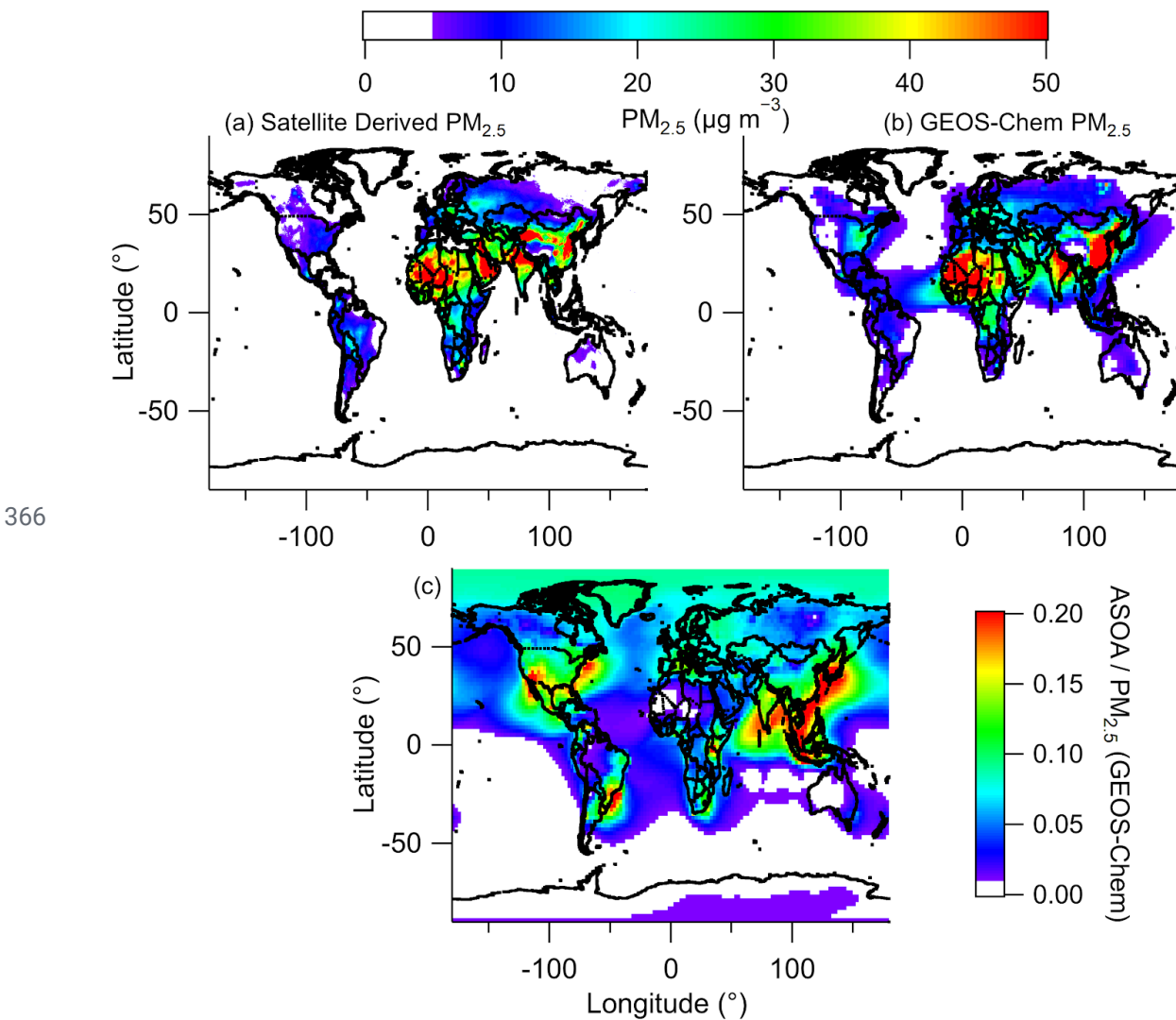
Figure S9. Comparison of satellite retrieved $PM_{2.5}$ (upper left) versus modeled $PM_{2.5}$ (upper right). (Bottom) Fractional contribution of ASOA to total modeled $PM_{2.5}$.
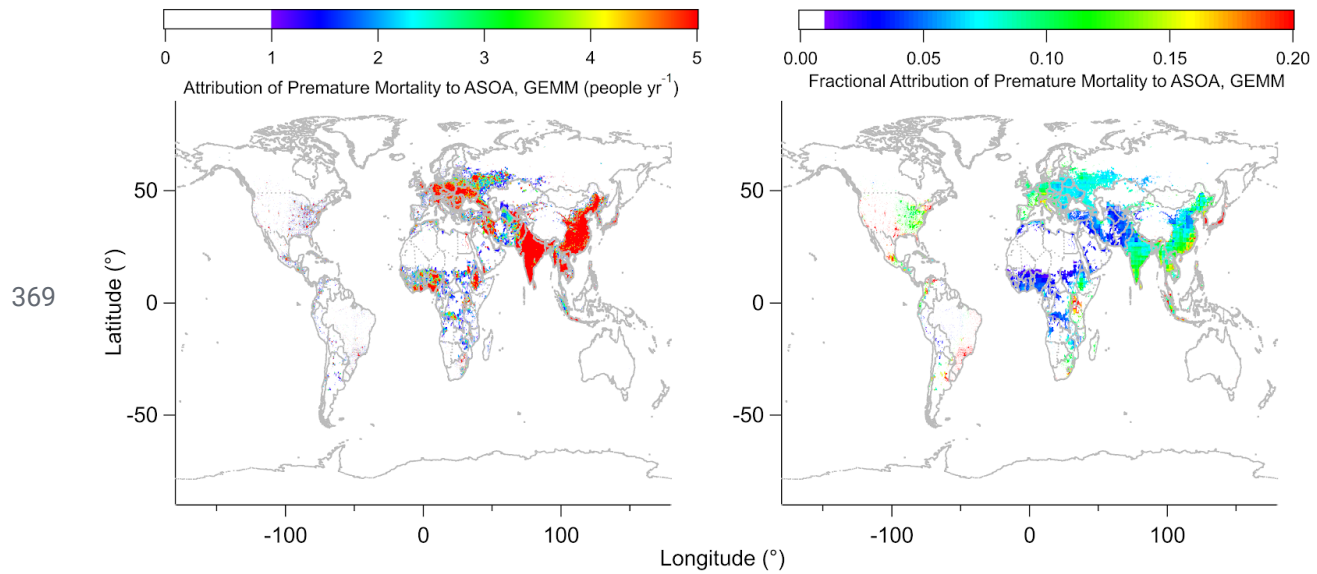
Figure S10. Same as Fig. S8, but using the GEMM from Burnett et al. (2018). (top). (Left) Attribution of premature mortality to ASOA per 10×10 km^2 area (people yr^{-1}) and (Right) fractional attribution of preamture mortality to ASOA per 10×10^2 km for one year.

Figure S11. Same as Fig. S10 but summed up for each country for the (left) attribution of premature mortality to ASOA (people yr^{-1}) and (right) the fractional attribution of premature mortality to ASOA for one year.

Figure S12. Comparison for surface level ozone upon reducing SOA precursors by 20%.
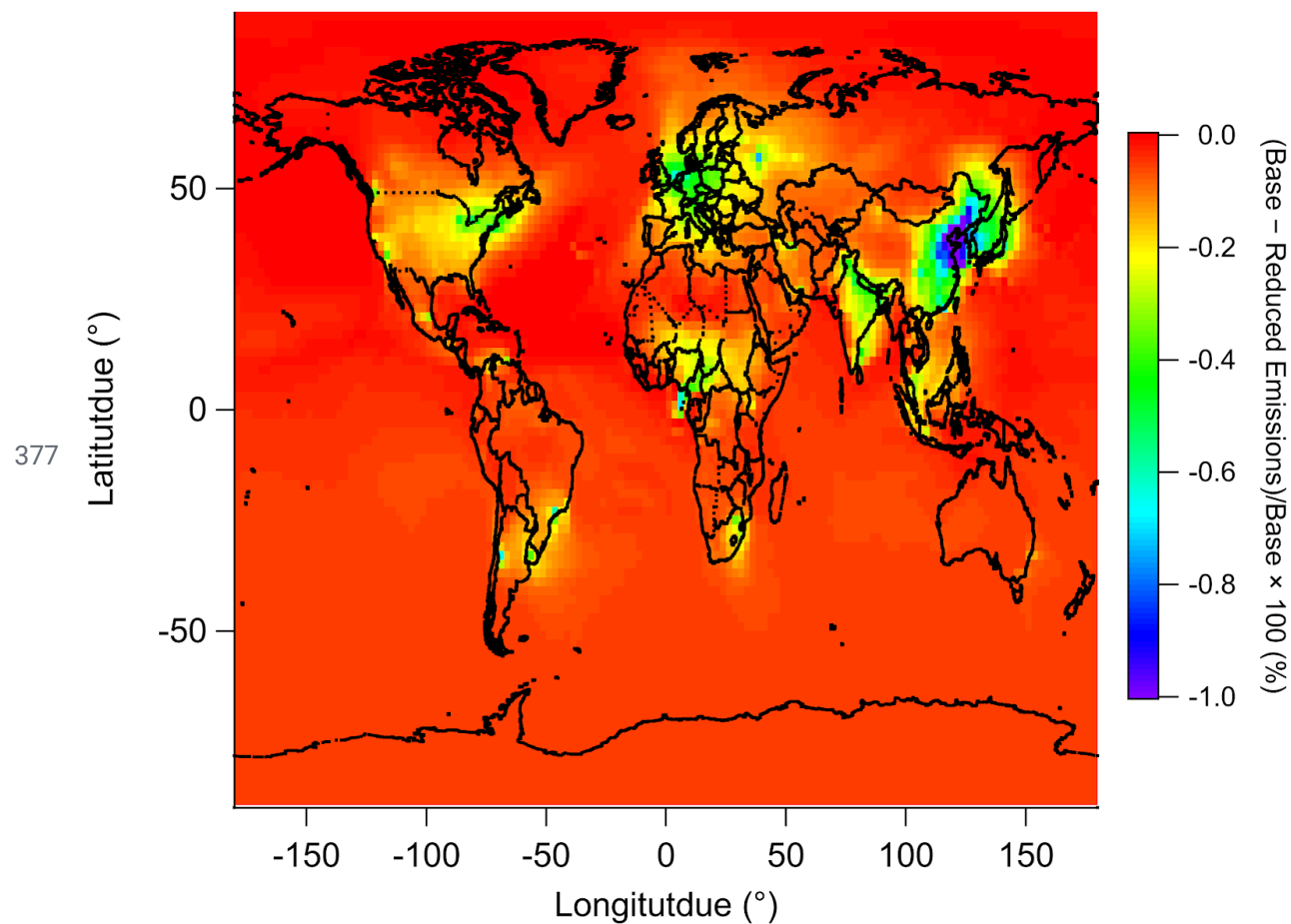
References

Apel, E. C., Emmons, L. K., Karl, T., Flocke, F., Hills, a. J., Madronich, S., Lee-Taylor, J., Fried, A., Weibring, P., Walega, J., Richter, D., Tie, X., Mauldin, L., Campos, T., Weinheimer, A., Knapp, D., Sive, B., Kleinman, L., Springston, S., Zaveri, R., Ortega, J., Voss, P., Blake, D., Baker, A., Warneke, C., Welsh-Bon, D., de Gouw, J., Zheng, J., Zhang, R., Rudolph, J., Junkermann, W. and Riemer, D. D.: Chemical evolution of volatile organic compounds in the outflow of the Mexico City Metropolitan area, Atmos. Chem. Phys., 10(5), 2353–2375, 2010.

Atkinson, R. and Arey, J.: Atmospheric Degradation of Volatile Organic Compounds, Chem. Rev., 103, 4605–4638, 2003.

Atkinson, R., Baulch, D. L., Cox, R. A., Crowley, J. N., Hampson, R. F., Hynes, R. G., Jenkin, M. E., Rossi, M. J., Troe, J. and IUPAC Subcommittee: Evaluated kinetic and photochemical data for atmospheric chemistry: Volume II - gas phase reactions of organic species, Atmos. Chem. Phys., 6(11), 3625–4055, 2006.

Baker, A. K., Beyersdorf, A. J., Doezema, L. A., Katzenstein, A., Meinardi, S., Simpson, I. J., Blake, D. R. and Sherwood Rowland, F.: Measurements of nonmethane hydrocarbons in 28 United States cities, Atmos. Environ., 42(1), 170–182, 2008.

Blake, N. J., Blake, D. R., Simpson, I. J., Meinardi, S., Swanson, A. L., Lopez, J. P., Katzenstein, A. S., Barletta, B., Shirai, T., Atlas, E., Sachse, G., Avery, M., Vay, S., Fuelberg, H. E., Kiley, C. M., Kita, K. and Rowland, F. S.: NMHCs and halocarbons in Asian continental outflow during the Transport and Chemical Evolution over the Pacific (TRACE-P) Field Campaign: Comparison with PEM-West B, Journal of Geophysical Research-Atmospheres, 108(D20), 8806, 2003.

Bohn, B. and Zetzsch, C.: Kinetics and mechanism of the reaction of OH with the trimethylbenzenes – experimental evidence for the formation of adduct isomers, Phys. Chem. Chem. Phys., 14(40), 13933, 2012.

Burnett, R., Chen, H., Szyszkowicz, M., Fann, N., Hubbell, B., Pope, C. A., Apte, J. S., Brauer, M., Cohen, A., Weichenthal, S., Coggins, J., Di, Q., Brunekreef, B., Frostad, J., Lim, S. S., Kan, H., Walker, K. D., Thurston, G. D., Hayes, R. B., Lim, C. C., Turner, M. C., Jerrett, M., Krewski, D., Gapstur, S. M., Diver, W. R., Ostro, B., Goldberg, D., Crouse, D. L., Martin, R. V., Peters, P., Pinault, L., Tjepkema, M., van Donkelaar, A., Villeneuve, P. J., Miller, A. B., Yin, P., Zhou, M., Wang, L., Janssen, N. A. H., Marra, M., Atkinson, R. W., Tsang, H., Quoc Thach, T., Cannon, J. B., Allen, R. T., Hart, J. E., Laden, F., Cesaroni, G., Forastiere, F., Weinmayr, G., Jaensch, A., Nagel, G., Concin, H. and Spadaro, J. V.: Global estimates of mortality associated with long-term exposure to outdoor fine particulate matter, Proc. Natl. Acad. Sci. U. S. A., 115(38), 9592–9597, 2018.

Burnett, R. T., Pope, C. A., Ezzati, M., Olives, C., Lim, S. S., Mehta, S., Shin, H. H., Singh, G., Hubbell, B., Brauer, M., Anderson, H. R., Smith, K. R., Balmes, J. R., Bruce, N. G., Kan, H., Laden, F., Prüss-Ustün, A., Turner, M. C., Gapstur, S. M., Diver, W. R. and Cohen, A.: An integrated risk function for estimating the global burden of disease attributable to ambient fine

particulate matter exposure, Environ. Health Perspect., 122(4), 397–403, 2014.

CARB: CEPAM: 2013 Almanac - Standard Emissions Tool, [online] Available from: https://www.arb.ca.gov/app/emsinv/fcemssumcat2013.php, 2013.

Cárdenas, L. M., Brassington, D. J., Allan, B. J., Coe, H., Alicke, B., Platt, U., Wilson, K. M., Plane, J. M. C. and Penkett, S. A.: Intercomparison of Formaldehyde Measurements in Clean and Polluted Atmospheres, J. Atmos. Chem., 37(1), 53–80, 2000.

Cazorla, M., Wolfe, G. M., Bailey, S. A., Swanson, A. K., Arkinson, H. L. and Hanisco, T. F.: A new airborne laser-induced fluorescence instrument for in situ detection of formaldehyde throughout the troposphere and lower stratosphere, Atmos. Meas. Tech., 8(2), 541–552, 2015.

CCPR: The California Consumer Products Regulation., 2015.

Davis, M. S.: 2005 Architectural Coatings Survey Final Report, CARB., 2007.

DeCarlo, P. F., Kimmel, J. R., Trimborn, A., Northway, M. J., Jayne, J. T., Aiken, A. C., Gonin, M., Fuhrer, K., Horvath, T., Docherty, K. S., Worsnop, D. R. and Jimenez, J. L.: Field-deployable, high-resolution, time-of-flight aerosol mass spectrometer, Anal. Chem., 78(24), 8281–8289, 2006.

DeCarlo, P. F., Ulbrich, I. M., Crounse, J., de Foy, B., Dunlea, E. J., Aiken, A. C., Knapp, D., Weinheimer, A. J., Campos, T., Wennberg, P. O. and Jimenez, J. L.: Investigation of the sources and processing of organic aerosol over the Central Mexican Plateau from aircraft measurements during MILAGRO, Atmos. Chem. Phys., 10(12), 5257–5280, 2010.

van Donkelaar, A., Martin, R. V., Brauer, M., Hsu, N. C., Kahn, R. A., Levy, R. C., Lyapustin, A., Sayer, A. M. and Winker, D. M.: Global Estimates of Fine Particulate Matter using a Combined Geophysical-Statistical Method with Information from Satellites, Models, and Monitors, Environ. Sci. Technol., 50(7), 3762–3772, 2016.

Drewnick, F., Hings, S. S., DeCarlo, P., Jayne, J. T., Gonin, M., Fuhrer, K., Weimer, S., Jimenez, J. L., Demerjian, K. L., Borrmann, S. and Worsnop, D. R.: A New Time-of-Flight Aerosol Mass Spectrometer (TOF-AMS)—Instrument Description and First Field Deployment, Aerosol Sci. Technol., 39(7), 637–658, 2005.

Dunmore, R. E., Hopkins, J. R., Lidster, R. T., Lee, J. D., Evans, M. J., Rickard, A. R., Lewis, A. C. and Hamilton, J. F.: Diesel-related hydrocarbons can dominate gas phase reactive carbon in megacities, Atmos. Chem. Phys., 15, 9983–9996, 2015.

EMEP/EEA: EMEP/EEA Air Pollutant Emission Inventory Guidebook 2016, EEA, Luxembourg., 2016.

EPA: SPECIATE v4.4, US Environmental Protection Agency., 2014.

Fisher, J. A., Jacob, D. J., Travis, K. R., Kim, P. S., Marais, E. A., Miller, C. C., Yu, K., Zhu, L.,

Yantosca, R. M., Sulprizio, M. P., Mao, J., Wennberg, P. O., Crounse, J. D., Teng, A. P., Nguyen, T. B., Clair, J. M. S., Cohen, R. C., Romer, P., Nault, B. A., Wooldridge, P. J., Jimenez, J. L., Campuzano-Jost, P., Day, D. A., Hu, W., Shepson, P. B., Xiong, F., Blake, D. R., Goldstein, A. H., Misztal, P. K., Hanisco, T. F., Wolfe, G. M., Ryerson, T. B., Wisthaler, A. and Mikoviny, T.: Organic nitrate chemistry and its implications for nitrogen budgets in an isoprene- and monoterpene-rich atmosphere: Constraints from aircraft (SEAC[4]RS) and ground-based (SOAS) observations in the Southeast US, Atmos. Chem. Phys., 16(9), doi:10.5194/acp-16-5969-2016, 2016.

Fried, A., Crawford, J., Olson, J., Walega, J., Potter, W., Wert, B., Jordan, C., Anderson, B., Shetter, R., Lefer, B., Blake, D., Blake, N., Meinardi, S., Heikes, B., O'Sullivan, D., Snow, J., Fuelberg, H., Kiley, C. M., Sandholm, S., Tan, D., Sachse, G., Singh, H., Faloona, I., Harward, C. N. and Carmichael, G. R.: Airborne tunable diode laser measurements of formaldehyde during TRACE-P: Distributions and box model comparisons, J. Geophys. Res. D: Atmos., 108(D20), 8798, 2003.

Gately, C. K., Hutyra, L. R. and Wing, I. S.: Cities, traffic, and CO_2: A multidecadal assessment of trends, drivers, and scaling relationships, Proc. Natl. Acad. Sci. U. S. A., 112(16), 4999–5004, 2015.

Gentner, D. R., Isaacman, G., Worton, D. R., Chan, A. W. H., Dallmann, T. R., Davis, L., Liu, S., Day, D. A., Russell, L. M., Wilson, K. R., Weber, R., Guha, A., Harley, R. A. and Goldstein, A. H.: Elucidating secondary organic aerosol from diesel and gasoline vehicles through detailed characterization of organic carbon emissions, Proc. Natl. Acad. Sci. U. S. A., 109(45), 18318–18323, 2012.

Gentner, D. R., Worton, D. R., Isaacman, G., Davis, L. C., Dallmann, T. R., Wood, E. C., Herndon, S. C., Goldstein, A. H. and Harley, R. A.: Chemical Composition of Gas-Phase Organic Carbon Emissions from Motor Vehicles and Implications for Ozone Production, Environ. Sci. Technol., 47(20), 11837–11848, 2013.

Gerbig, C., Schmitgen, S., Kley, D., Volz-Thomas, A., Dewey, K. and Haaks, D.: An improved fast-response vacuum-UV resonance fluorescence CO instrument, J. Geophys. Res. D: Atmos., 104(D1), 1699–1704, 1999.

Gilman, J. B., Burkhart, J. F., Lerner, B. M., Williams, E. J., Kuster, W. C., Goldan, P. D., Murphy, P. C., Warneke, C., Fowler, C., Montzka, S. A., Miller, B. R., Miller, L., Oltmans, S. J., Ryerson, T. B., Cooper, O. R., Stohl, A. and de Gouw, J. A.: Ozone variability and halogen oxidation within the Arctic and sub-Arctic springtime boundary layer, Atmos. Chem. Phys., 10(21), 10223–10236, 2010.

de Gouw, J. A., Middlebrook, A. M., Warneke, C., Goldan, P. D., Kuster, W. C., Roberts, J. M., Fehsenfeld, F. C., Worsnop, D. R., Canagaratna, M. R., Pszenny, A. A. P., Keene, W. C., Marchewka, M., Bertman, S. B. and Bates, T. S.: Budget of organic carbon in a polluted atmosphere: Results from the New England Air Quality Study in 2002, J. Geophys. Res. D:

Atmos., 110(16), 1–22, 2005.

de Gouw, J. A., Gilman, J. B., Kim, S.-W., Lerner, B. M., Isaacman-VanWertz, G., McDonald, B. C., Warneke, C., Kuster, W. C., Lefer, B. L., Griffith, S. M., Dusanter, S., Stevens, P. S. and Stutz, J.: Chemistry of Volatile Organic Compounds in the Los Angeles basin: Nighttime Removal of Alkenes and Determination of Emission Ratios, J. Geophys. Res.: Atmos., 122(21), 11,843–11,861, 2017.

Griffith, S. M., Hansen, R. F., Dusanter, S., Michoud, V., Gilman, J. B., Kuster, W. C., Veres, P. R., Graus, M., Gouw, J. A., Roberts, J., Young, C., Washenfelder, R., Brown, S. S., Thalman, R., Waxman, E., Volkamer, R., Tsai, C., Stutz, J., Flynn, J. H., Grossberg, N., Lefer, B., Alvarez, S. L., Rappenglueck, B., Mielke, L. H., Osthoff, H. D. and Stevens, P. S.: Measurements of hydroxyl and hydroperoxy radicals during CalNex-LA: Model comparisons and radical budgets, J. Geophys. Res. D: Atmos., 121(8), 4211–4232, 2016.

Hassler, B., McDonald, B. C., Frost, G. J., Borbon, A., Carslaw, D. C., Civerolo, K., Granier, C., Monks, P. S., Monks, S., Parrish, D. D., Pollack, I. B., Rosenlof, K. H., Ryerson, T. B., von Schneidemesser, E. and Trainer, M.: Analysis of long-term observations of NO_x and CO in megacities and application to constraining emissions inventories, Geophys. Res. Lett., 43(18), 9920–9930, 2016.

Hayes, P. L., Ortega, A. M., Cubison, M. J., Froyd, K. D., Zhao, Y., Cliff, S. S., Hu, W. W., Toohey, D. W., Flynn, J. H., Lefer, B. L., Grossberg, N., Alvarez, S., Rappenglück, B., Taylor, J. W., Allan, J. D., Holloway, J. S., Gilman, J. B., Kuster, W. C., de Gouw, J. A., Massoli, P., Zhang, X., Liu, J., Weber, R. J., Corrigan, A. L., Russell, L. M., Isaacman, G., Worton, D. R., Kreisberg, N. M., Goldstein, A. H., Thalman, R., Waxman, E. M., Volkamer, R., Lin, Y. H., Surratt, J. D., Kleindienst, T. E., Offenberg, J. H., Dusanter, S., Griffith, S., Stevens, P. S., Brioude, J., Angevine, W. M. and Jimenez, J. L.: Organic aerosol composition and sources in Pasadena, California, during the 2010 CalNex campaign, J. Geophys. Res. D: Atmos., 118(16), 9233–9257, 2013.

Huey L Tanner D Slusher D Dibb J Arimoto R Chen G Davis D Buhr M Nowak J Mauldin R Eisele F, K. E.: CIMS measurements of HNO3 and SO2 at the South Pole during ISCAT 2000, Atmos. Environ., 38(32), 5411–5421, 2004.

Hu, W., Hu, M., Hu, W., Jimenez, J. L., Yuan, B., Chen, W., Wang, M., Wu, Y., Chen, C., Wang, Z., Peng, J., Zeng, L. and Shao, M.: Chemical composition, sources, and aging process of submicron aerosols in Beijing: Contrast between summer and winter, J. Geophys. Res. D: Atmos., 121(4), 1955–1977, 2016.

IEA: World energy balances, IEA World Energy Statistics and Balances, doi:10.1787/data-00521-en, 2019.

Janssens-Maenhout, G., Crippa, M., Guizzardi, D., Dentener, F., Muntean, M., Pouliot, G., Keating, T., Zhang, Q., Kurokawa, J., Wankmüller, R., Denier van der Gon, H., Kuenen, J. J. P., Klimont, Z., Frost, G., Darras, S., Koffi, B. and Li, M.: HTAP_v2.2: a mosaic of regional and

global emission grid maps for 2008 and 2010 to study hemispheric transport of air pollution, Atmos. Chem. Phys., 15(19), 11411–11432, 2015.

Jayne, J. T., Leard, D. C., Zhang, X. F., Davidovits, P., Smith, K. A., Kolb, C. E. and Worsnop, D. R.: Development of an aerosol mass spectrometer for size and composition analysis of submicron particles, Aerosol Sci. Technol., 33(1-2), 49–70, 2000.

Kaiser, J., Jacob, D. J., Zhu, L., Travis, K. R., Fisher, J. A., González Abad, G., Zhang, L., Zhang, X., Fried, A., Crounse, J. D., St. Clair, J. M. and Wisthaler, A.: High-resolution inversion of OMI formaldehyde columns to quantify isoprene emission on ecosystem-relevant scales: application to the southeast US, Atmos. Chem. Phys., 18(8), 5483–5497, 2018.

Kim, S., Huey, L. G., Stickel, R. E., Tanner, D. J., Crawford, J. H., Olson, J. R., Chen, G., Brune, W. H., Ren, X., Lesher, R., Wooldridge, P. J., Bertram, T. H., Perring, A., Cohen, R. C., Lefer, B. L., Shetter, R. E., Avery, M., Diskin, G. and Sokolik, I.: Measurement of HO_2NO_2 in the free troposphere during the Intercontinental Chemical Transport Experiment–North America 2004, J. Geophys. Res. D: Atmos., 112, D12S01, 2007.

Kleinman, L. I., Daum, P. H., Lee, Y.-N., Senum, G. I., Springston, S. R., Wang, J., Berkowitz, C., Hubbe, J., Zaveri, R. A., Brechtel, F. J., Jayne, J., Onasch, T. B. and Worsnop, D.: Aircraft observations of aerosol composition and ageing in New England and Mid-Atlantic States during the summer 2002 New England Air Quality Study field campaign, J. Geophys. Res. D: Atmos., 112(D9), D09310, 2007.

Langford, B., Nemitz, E., House, E., Phillips, G. J., Famulari, D., Davison, B., Hopkins, J. R., Lewis, A. C. and Hewitt, C. N.: Fluxes and concentrations of volatile organic compounds above central London, UK, Atmos. Chem. Phys., 10(2), 627–645, 2010.

Li, M., Zhang, Q., Streets, D. G., He, K. B., Cheng, Y. F., Emmons, L. K., Huo, H., Kang, S. C., Lu, Z., Shao, M., Su, H., Yu, X. and Zhang, Y.: Mapping Asian anthropogenic emissions of non-methane volatile organic compounds to multiple chemical mechanisms, Atmos. Chem. Phys., 14(11), 5617–5638, 2014.

Li, M., Liu, H., Geng, G., Hong, C., Liu, F., Song, Y., Tong, D., Zheng, B., Cui, H., Man, H., Zhang, Q. and He, K.: Anthropogenic emission inventories in China: a review, Natl Sci Rev, 4(6), 834–866, 2017.

Li, M., Zhang, Q., Zheng, B., Tong, D., Lei, Y., Liu, F., Chaopeng, H., Kang, S., Yan, L., Zhang, Y., Bo, Y., Su, H., Cheng, Y. and He, K.: Persistent growth of anthropogenic non-methane volatile organic compound (NMVOC) emissions in China during 1990-2017: drivers, speciation and ozone formation potential, Atmos. Chem. Phys., 19, 8897–8913, 2019.

Liu, F., Zhang, Q., Tong, D., Zheng, B., Li, M., Huo, H. and He, K. B.: High-resolution inventory of technologies, activities, and emissions of coal-fired power plants in China from 1990 to 2010, Atmos. Chem. Phys., 15(23), 13299–13317, 2015.

Marais, E. A., Jacob, D. J., Jimenez, J. L., Campuzano-Jost, P., Day, D. A., Hu, W., Krechmer, J.,

Zhu, L., Kim, P. S., Miller, C. C., Fisher, J. A., Travis, K., Yu, K., Hanisco, T. F., Wolfe, G. M., Arkinson, H. L., Pye, H. O. T., Froyd, K. D., Liao, J. and McNeill, V. F.: Aqueous-phase mechanism for secondary organic aerosol formation from isoprene: application to the southeast United States and co-benefit of SO_2 emission controls, Atmos. Chem. Phys., 16(3), 1603–1618, 2016.

Matheson, R. R.: 20th- to 21st-Century Technological Challenges in Soft Coatings, Science, 297(5583), 976–979, 2002.

McDonald, B. C., Gentner, D. R., Goldstein, A. H. and Harley, R. A.: Long-Term Trends in Motor Vehicle Emissions in U.S. Urban Areas, Environ. Sci. Technol., 47(17), 10022–10031, 2013.

McDonald, B. C., Goldstein, A. H. and Harley, R. A.: Long-Term Trends in California Mobile Source Emissions and Ambient Concentrations of Black Carbon and Organic Aerosol, Environ. Sci. Technol., 49(8), 5178–5188, 2015.

McDonald, B. C., de Gouw, J. A., Gilman, J. B., Jathar, S. H., Akherati, A., Cappa, C. D., Jimenez, J. L., Lee-Taylor, J., Hayes, P. L., McKeen, S. A., Cui, Y. Y., Kim, S.-W., Gentner, D. R., Isaacman-VanWertz, G., Goldstein, A. H., Harley, R. A., Frost, G. J., Roberts, J. M., Ryerson, T. B. and Trainer, M.: Volatile chemical products emerging as largest petrochemical source of urban organic emissions, Science, 359(6377), 760–764, 2018.

Mollner, A. K., Valluvadasan, S., Feng, L., Sprague, M. K., Okumura, M., Milligan, D. B., Bloss, W. J., Sander, S. P., Martien, P. T., Harley, R. A., McCoy, A. B. and Carter, W. P. L.: Rate of Gas Phase Association of Hydroxyl Radical and Nitrogen Dioxide, Science, 330(6004), 646–649, 2010.

MOVES: MOVES2014a User Guide., 2015.

NEI: National Emissions Inventory (NEI) 2011, version 1, Research Triangle Park., 2015.

Pai, S. J., Heald, C. L., Pierce, J. R., Farina, S. C., Marais, E. A., Jimenez, J. L., Campuzano-Jost, P., Nault, B. A., Middlebrook, A. M., Coe, H., Shilling, J. E., Bahreini, R., Dingle, J. H. and Vu, K.: An evaluation of global organic aerosol schemes using airborne observations, Atmos. Chem. Phys., 20(5), 2637–2665, 2020.

Pierson, W. R., Schorran, D. E., Fujita, E. M., Sagebiel, J. C., Lawson, D. R. and Tanner, R. L.: Assessment of Nontailpipe Hydrocarbon Emissions from Motor Vehicles, J. Air Waste Manage. Assoc., 49(5), 498–519, 1999.

Pollack, I. B., Lerner, B. M. and Ryerson, T. B.: Evaluation of ultraviolet light-emitting diodes for detection of atmospheric NO_2 by photolysis - chemiluminescence, J. Atmos. Chem., 65(2-3), 111–125, 2010.

Roberts, J. M., Stroud, C. A., Jobson, B. T., Trainer, M., Hereid, D., Williams, E., Fehsenfeld, F., Brune, W., Martinez, M. and Harder, H.: Application of a sequential reaction model to PANs and

aldehyde measurements in two urban areas, Geophys. Res. Lett., 28(24), 4583–4586, 2001.

Roberts, J. M., Flocke, F., Stroud, C. A., Hereid, D., Williams, E., Fehsenfeld, F., Brune, W., Martinez, M. and Harder, H.: Ground-based measurements of peroxycarboxylic nitric anhydrides (PANs) during the 1999 Southern Oxidants Study Nashville Intensive, J. Geophys. Res. D: Atmos., 107(D21), 4554, 2002.

Rubin, J. I., Kean, A. J., Harley, R. A., Millet, D. B. and Goldstein, A. H.: Temperature dependence of volatile organic compound evaporative emissions from motor vehicles, J. Geophys. Res. D: Atmos., 111(D3), D03305, 2006.

Ryerson, T. B., Huey, L. G., Knapp, K., Neuman, J. A., Parrish, D. D., Sueper, D. T. and Fehsenfeld, F. C.: Design and initial characterization of an inlet for gas-phase NO_y measurements from aircraft, J. Geophys. Res. D: Atmos., 104(D5), 5483–5492, 1999.

Ryerson, T. B., Andrews, A. E., Angevine, W. M., Bates, T. S., Brock, C. A., Cairns, B., Cohen, R. C., Cooper, O. R., de Gouw, J. A., Fehsenfeld, F. C., Ferrare, R. A., Fischer, M. L., Flagan, R. C., Goldstein, A. H., Hair, J. W., Hardesty, R. M., Hostetler, C. A., Jimenez, J. L., Langford, A. O., McCauley, E., McKeen, S. A., Molina, L. T., Nenes, A., Oltmans, S. J., Parrish, D. D., Pederson, J. R., Pierce, R. B., Prather, K., Quinn, P. K., Seinfeld, J. H., Senff, C. J., Sorooshian, A., Stutz, J., Surratt, J. D., Trainer, M., Volkamer, R., Williams, E. J. and Wofsy, S. C.: The 2010 California Research at the Nexus of Air Quality and Climate Change (CalNex) field study, J. Geophys. Res. D: Atmos., 118(11), 5830–5866, 2013.

Sachse, G. W., Hill, G. F., Wade, L. O. and Perry, M. G.: Fast-Response, High-Precision Carbon Monoxide Sensor using a Tunable Diode Laser Absorption Technique, J. Geophys. Res.: Atmos., 92(D2), 2071–2081, 1987.

Schroder, J. C., Campuzano-Jost, P., Day, D. A., Shah, V., Larson, K., Sommers, J. M., Sullivan, A. P., Campos, T., Reeves, J. M., Hills, A., Hornbrook, R. S., Blake, N. J., Scheuer, E., Guo, H., Fibiger, D. L., McDuffie, E. E., Hayes, P. L., Weber, R. J., Dibb, J. E., Apel, E. C., Jaeglé, L., Brown, S. S., Thronton, J. A. and Jimenez, J. L.: Sources and Secondary Production of Organic Aerosols in the Northeastern US during WINTER, J. Geophys. Res. D: Atmos., doi:10.1029/2018JD028475, 2018.

Simon, H., Beck, L., Bhave, P. V., Divita, F., Hsu, Y., Luecken, D., Mobley, J. D., Pouliot, G. A., Reff, A., Sarwar, G. and Strum, M.: The development and uses of EPA's SPECIATE database, Atmos. Pollut. Res., 1(4), 196–206, 2010.

Slusher, D. L., Huey, L. G., Tanner, D. J., Flocke, F. M. and Roberts, J. M.: A thermal dissociation-chemical ionization mass spectrometry (TD-CIMS) technique for the simultaneous measurement of peroxyacyl nitrates and dinitrogen pentoxide, J. Geophys. Res.: Atmos., 109(D19), D19315–D19315, 2004.

Stutz, J. and Platt, U.: Numerical analysis and estimation of the statistical error of differential optical absorption spectroscopy measurements with least-squares methods, Appl. Opt., 35(30),

637 6041, 1996.

638 Stutz, J. and Platt, U.: Improving long-path differential optical absorption spectroscopy with a
639 quartz-fiber mode mixer, Appl. Opt., 36(6), 1105, 1997.

640 Travis, K. R., Jacob, D. J., Fisher, J. A., Kim, P. S., Marais, E. A., Zhu, L., Yu, K., Miller, C. C.,
641 Yantosca, R. M., Sulprizio, M. P., Thompson, A. M., Wennberg, P. O., Crounse, J. D., St. Clair, J.
642 M., Cohen, R. C., Laughner, J. L., Dibb, J. E., Hall, S. R., Ullmann, K., Wolfe, G. M., Pollack, I.
643 B., Peischl, J., Neuman, J. A. and Zhou, X.: Why do models overestimate surface ozone in the
644 Southeast United States?, Atmos. Chem. Phys., 16(21), 13561–13577, 2016.

645 Vaughan, A. R., Lee, J. D., Shaw, M. D., Misztal, P. K., Metzger, S., Vieno, M., Davison, B.,
646 Karl, T. G., Carpenter, L. J., Lewis, A. C., Purvis, R. M., Goldstein, A. H. and Hewitt, C. N.:
647 VOC emission rates over London and South East England obtained by airborne eddy covariance,
648 Faraday Discuss., 200(0), 599–620, 2017.

649 Wang, M., Shao, M., Chen, W., Yuan, B., Lu, S., Zhang, Q., Zeng, L. and Wang, Q.: A
650 temporally and spatially resolved validation of emission inventories by measurements of ambient
651 volatile organic compounds in Beijing, China, Atmos. Chem. Phys., 14(12), 5871–5891, 2014.

652 Warneke, C., McKeen, S. A., de Gouw, J. A., Goldan, P. D., Kuster, W. C., Holloway, J. S.,
653 Williams, E. J., Lerner, B. M., Parrish, D. D., Trainer, M., Fehsenfeld, F. C., Kato, S., Atlas, E.
654 L., Baker, A. and Blake, D. R.: Determination of urban volatile organic compound emission
655 ratios and comparison with an emissions database, J. Geophys. Res. D: Atmos., 112(D10),
656 doi:10.1029/2006JD007930, 2007.

657 Warneke, C., Veres, P., Holloway, J. S., Stutz, J., Tsai, C., Alvarez, S., Rappenglueck, B.,
658 Fehsenfeld, F. C., Graus, M., Gilman, J. B. and de Gouw, J. A.: Airborne formaldehyde
659 measurements using PTR-MS: calibration, humidity dependence, inter-comparison and initial
660 results, Atmos. Meas. Tech., 4(10), 2345–2358, 2011.

661 Warneke, C., de Gouw, J. A., Holloway, J. S., Peischl, J., Ryerson, T. B., Atlas, E., Blake, D.,
662 Trainer, M. and Parrish, D. D.: Multiyear trends in volatile organic compounds in Los Angeles,
663 California: Five decades of decreasing emissions, J. Geophys. Res. D: Atmos., 117(D21),
664 D00V17, 2012.

665 Weibring, P., Richter, D., Walega, J. G., Rippe, L. and Fried, A.: Difference frequency generation
666 spectrometer for simultaneous multispecies detection, Opt. Express, 18(26), 27670, 2010.

667 Weinheimer, A. J., Walega, J. G., Ridley, B. A., Gary, B. L., Blake, D. R., Blake, N. J., Rowland,
668 F. S., Sachse, G. W., Anderson, B. E. and Collins, J. E.: Meridional distributions of NO_x, NO_y,
669 and other species in the lower stratosphere and upper troposphere during AASE II, Geophys.
670 Res. Lett., 21(23), 2583–2586, 1994.

671 Whalley, L. K., Stone, D., Bandy, B., Dunmore, R., Hamilton, J. F., Hopkins, J., Lee, J. D.,
672 Lewis, A. C. and Heard, D. E.: Atmospheric OH reactivity in central London: observations,
673 model predictions and estimates of in situ ozone production, Atmos. Chem. Phys., 16(4),

2109–2122, 2016.

Williams, E. J., Roberts, J. M., Baumann, K., Bertman, S. B., Buhr, S., Norton, R. B. and Fehsenfeld, F. C.: Variations in NO_y composition at Idaho Hill, Colorado, J. Geophys. Res. D: Atmos., 102(D5), 6297–6314, 1997.

Williams, J., Roberts, J. M., Bertman, S. B., Stroud, C. A., Fehsenfeld, F. C., Baumann, K., Buhr, M. P., Knapp, K., Murphy, P. C., Nowick, M. and Williams, E. J.: A method for the airborne measurement of PAN, PPN, and MPAN, J. Geophys. Res. D: Atmos., 105(D23), 28943–28960, 2000.

Young, D. E., Allan, J. D., Williams, P. I., Green, D. C., Flynn, M. J., Harrison, R. M., Yin, J., Gallagher, M. W. and Coe, H.: Investigating the annual behaviour of submicron secondary inorganic and organic aerosols in London, Atmos. Chem. Phys., 15, 6351–6366, 2015.

Yuan, B., Hu, W. W., Shao, M., Wang, M., Chen, W. T., Lu, S. H., Zeng, L. M. and Hu, M.: VOC emissions, evolutions and contributions to SOA formation at a receptor site in eastern China, Atmos. Chem. Phys., 13(17), 8815–8832, 2013.

Zhang, Q., Streets, D. G., Carmichael, G. R., He, K. B., Huo, H., Kannari, A., Klimont, Z., Park, I. S., Reddy, S., Fu, J. S., Chen, D., Duan, L., Lei, Y., Wang, L. T. and Yao, Z. L.: Asian emissions in 2006 for the NASA INTEX-B mission, Atmos. Chem. Phys., 9(14), 5131–5153, 2009.

Zheng, B., Huo, H., Zhang, Q., Yao, Z. L., Wang, X. T., Yang, X. F., Liu, H. and He, K. B.: High-resolution mapping of vehicle emissions in China in 2008, Atmos. Chem. Phys., 14(18), 9787–9805, 2014.

Zheng, B., Tong, D., Li, M., Liu, F., Hong, C., Geng, G., Li, H., Li, X., Peng, L., Qi, J., Yan, L., Zhang, Y., Zhao, H., Zheng, Y., He, K. and Zhang, Q.: Trends in China's anthropogenic emissions since 2010 as the consequence of clean air actions, Atmos. Chem. Phys., 18(19), 14095–14111, 2018.